European Journal of Medicinal Chemistry 69 (2013) 294–309

Contents lists available at ScienceDirect

European Journal of Medicinal Chemistry

journal homepage: http://www.elsevier.com/locate/ejmech

Original article

Design, synthesis, and *in vitro* cancer cell growth inhibition evaluation and antimalarial testing of trioxanes installed in cyclic 2-enoate substructures

Md. Imran Hossain [a], Marta Świtalska [b], Wei Peng [a], Mariko Takashima [a], Ning Wang [a], Marcel Kaiser [d,e], Joanna Wietrzyk [b,**], Shingo Dan [c,***], Takao Yamori [c], Tsutomu Inokuchi [a,*]

[a] Division of Chemistry and Biotechnology, Graduate School of Natural Science and Technology, Okayama University, 3-1-1 Tsushima-naka, Kita-ku, Okayama 700-8530, Japan
[b] Institute of Immunology and Experimental Therapy, Polish Academy of Sciences, 12 R. Weigl Street, 53-114 Wroclaw, Poland
[c] Division of Molecular Pharmacology, Cancer Chemotherapy Center, Japanese Foundation for Cancer Research, 3-8-31 Ariake, Koto-ku, Tokyo 135-8550, Japan
[d] Swiss Tropical and Public Health Institute, Socinstrasse 57, CH-4002 Basel, Switzerland
[e] University Basel, Petersplatz 1, CH-4003 Basel, Switzerland

ARTICLE INFO

Article history:
Received 11 April 2013
Received in revised form
30 July 2013
Accepted 2 August 2013
Available online 13 August 2013

Keywords:
Endoperoxides
1,2,4-Trioxanes
Anticancer agents
COMPARE study
Antimalarial

ABSTRACT

A novel series of 1,2,4-trioxanes were synthesized from 2*H*-pyrans via photooxidation, and their antiproliferative and growth factor inhibitory activity has been investigated across a variety of human cancer cell lines. Compounds **5k**, **5l**, **5s**, **7a** and **7c** exhibited the highest activity and selectivity against a human leukemia (MV4-11) cell line (IC_{50} = 0.5 μM). Compound **5o** showed the highest growth factor inhibitory activity against a melanoma (LOX-IMVI) cancer cell line (GI_{50} = 1.0 μM). A SAR study has confirmed the importance of the 1,2,4-trioxane unit as a pharmacophore for anticancer activity. The computer-assisted database analysis, COMPARE, has suggested that the compounds have unique mechanisms of actions that were different from those of known anticancer drugs. Some of the selected trioxanes were tested against the NF54 strain, albeit showing weak antiplasmodial activity. The molecular docking of trioxanes and hemin reveals that a short distance (1.30 Å) leads to their physical contact. The UV–vis spectroscopic analysis ensured the definite complexation between 1,2,4-trioxanes and hemin. The role of hemin –trioxane interaction in the hemin-induced oxidative damage has been studied using methylene blue as a substrate by UV–vis spectroscopy.

1. Introduction

Continuous drug resistances in tumors coupled with undesirable side effects in patients [1] have exposed the urgency of searching for new anticancer agents, particularly those with a novel and selective mechanism of action. The circumvention of these limitations has been directed to natural as well as synthetic sources [2,3]. Endoperoxides are found in the terpenes and their derivatives as secondary metabolites show biologically interesting activities. For example, as shown in Fig. 1, yingzhosu A, EDBD, arteflene, and okundoperoxide can kill malaria parasites at nanomolar concentrations while they exhibit cytotoxicity toward cancer-affected mammalian cells in the nanomolar to micromolar range [4–6]. Furthermore, the unique 1,2,4-trioxanes, the peroxygenated acetal-containing endoperoxide group, are considered today a relevant pharmacophore over a wide range of biological activities, as exemplified by well-known antimalarial drugs, arthemisinin and arterolane [7–9]. The removal of one oxygen or replacement of the peroxide group with an ether bridge from the 1,2,4-trioxanes significantly reduces the biological significance, proving the importance of the peroxide bridge [10–12]. The involvement of the 1,2,4-trioxane moiety in heme has been reported for its antimalarial activity [13], and the mode of action of 1,2,4-trioxane motifs for anticancer activity have also been examined [14]. The endoperoxide bridge that can be activated and fragmented with

* Corresponding author. Tel.: +81 86 251 8210; fax: +81 86 251 8021.
** Corresponding author. Tel.: +48 71 3709985; fax: +48 71 3371382.
*** Corresponding author. Tel.: +81 3 3520 0111; fax: +81 3 3570 0484.
E-mail addresses: wietrzyk@iitd.pan.wroc.pl (J. Wietrzyk), sdan@jfcr.or.jp (S. Dan), inokuchi@cc.okayama-u.ac.jp (T. Inokuchi).

0223-5234/$ – see front matter © 2013 Elsevier Masson SAS. All rights reserved.
http://dx.doi.org/10.1016/j.ejmech.2013.08.008

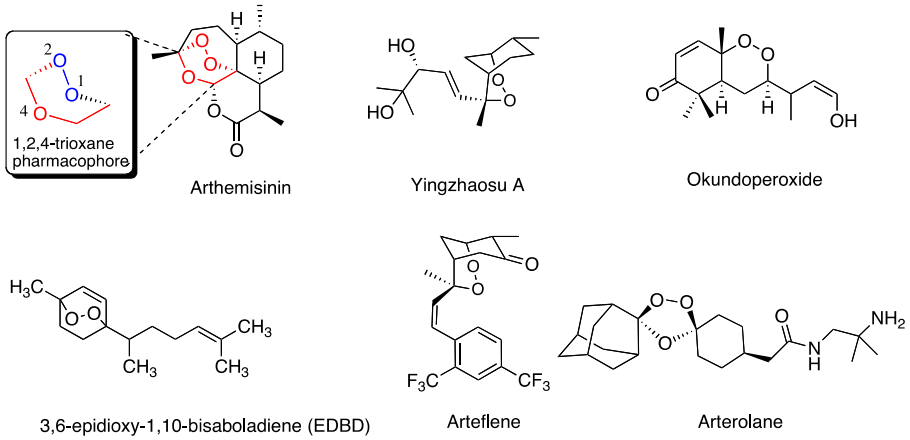

Fig. 1. Structure of some biologically important synthetic and natural endoperoxides.

intracellular iron [Fe(II)] leads to the formation of carbon-centered electrophilic radical species and reactive oxygen species (ROS) with involvement of Fenton chemistry [15]. Cancer cells undergoing rapid proliferation consume large quantities of the essential nutrient iron through up-regulation of the transferrin receptor, which might be directed to the similar action of mechanism against the *Plasmodium* parasite [16]. Although it is not a conventional biological target, heme is the master variable in the mechanism of action of peroxide-containing antimalarial drugs and could be a potential target for future anticancer drugs [14].

Recently, artemisinin-derived trioxane dimers were prepared and shown potent as anticancer chemotherapeutics [17–20]. Furthermore, fully synthetic 1,2,4-trioxane products were designed and shown to be promising for cancer growth inhibition [21]. Stimulated by these features, we have attempted to synthesize a new series of endoperoxides. Although target-based screening is now predominant, cell-based screening is still the main technique for unveiling cytotoxic drugs [22]. Therefore, we applied two-stage antiproliferative and cell growth inhibition activity tests. All of the derivatives are found to be active (IC_{50} = 0.5–13 μM) during the primary evaluation against human leukemia (MV4-11), human lung (A549), colon (HCT116) and normal murine fibroblast (BALB/3T3) cell lines. Some of the 1,2,4-trioxanes were examined for their antitumor effects across a panel of 39 human cancer cell lines, termed JFCR39, which comprised the subpanels of human cancer cell lines derived from breast, melanoma, lung, colon, central nervous system (CNS), ovary, stomach, kidney and prostate. An antitumor spectrum of each compound across JFCR39, or *fingerprint* was calculated and COMPARE analysis was carried out to predict the molecular mode of action of a respective antitumor compound by comparing the fingerprints with those of reference compounds possessing a known mechanism of action examined previously [23].

2. Results and discussion

2.1. Chemistry

The primary building blocks, polysubstituted 2*H*-pyrans **2a**–**d**, were prepared according to the reported method [24]. Subsequently, the peroxide installation was achieved via production of singlet oxygen with light and the sensitizer Rose bengal (Scheme 1), the data on which are listed in Table 1.

The preparation of the trioxanes **5a**–**w** is shown in Scheme 2 and results are listed in Table 2. The main scaffold, 2*H*-pyrans **4a**–**w**, was prepared by the sequence of condensation-6π-electrocyclization of **2** and α,β-unsaturated aldehydes, catalyzed by ethylene-1,2-ammonium diacetate (EDDA) [25]. The trioxanes **5a**–**w** were synthesized in a high yield by photooxidation of **4a**–**w** via generation of singlet oxygen utilizing a 250 W light bulb and the photo sensitizer Rose bengal (Scheme 2).

To confirm the structure of the bicyclic trioxane formed by this method, one of the isomers **5t** was subjected to an X-ray crystallographic analysis to determine its relative stereochemistry at the C2 and C7 positions (Fig. 2). As depicted, one of the isomers of **5t**, isolated by recrystallization, was unambiguously assigned to the 2,7-*cis* isomer based on the X-ray analysis.

7,7-Disubstituted trioxanes **8** were synthesized by the direct photooxidation of the corresponding crude 2*H*-pyrans **7** which were prepared from the 6,6-diphenyldihydro-2*H*-pyran-2,4(3*H*)-dione (**6**) and α,β-unsaturated aldehydes **1** according to Scheme 3, and the results are listed in Table 3.

The synthesis of trioxane in *N*-protected α,β-unsaturated amides **10a**–**d** is shown in Scheme 4, and the corresponding data are listed in Table 4. The amide analogs of trioxane were prepared by photooxidation of the respective 2*H*-pyrans **9** [25,26].

Finally, 1,3-cyclohexanediones were used to produce the respective 2*H*-pyrans **12a**–**d** according to the reported method [25], which are subsequently converted into their endoperoxide structures **13a**–**d** by photooxidation as shown in Scheme 5, and the antiproliferative activities thereof are listed in Table 5.

3. Pharmacology

3.1. Antiproliferative activity

The primary antiproliferative activity of the trioxanes was evaluated against four cell lines, i.e., human leukemia (MV4-11), lung (A549), colon (HCT116) and normal murine fibroblast (BALB/3T3) cell lines. The data for the *in vitro* anticancer activity are reported in Tables 1–5, expressed as the IC_{50}-concentration of the compound (in μM) that inhibits proliferation of the cells by 50%

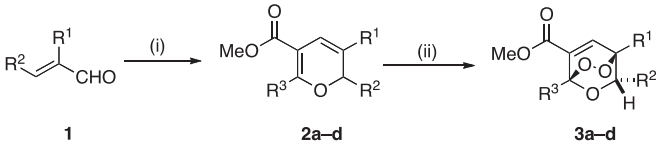

Scheme 1. Synthesis of 2,3,5-trioxabicyclo[2.2.2]oct-7-ene-8-carboxylate **3**. Reagent and conditions: (i) methyl 3-oxobutanoate, piperidine, AcOH, THP, rt, 24 h; (ii) Rose bengal, O_2, *hν*, MeOH, 0 °C, 1 h.

Table 1
Antiproliferative activity of **3a**–**d** against human leukemia MV4-11 cell line.

Entry	Compound	R^1	R^2	R^3	Yield (%)	MV4-11 IC_{50} (μM)
	Cisplatin					2.820 ± 0.450
1	**3a**	H_3C	H_3C	H_3C	85	>39
2	**3b**	H_3C	H_3C	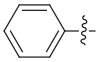	82	7.38 ± 0.37
3	**3c**		$R^1 = R^2$	H_3C	78	8.08 ± 2.90
4	**3d**	H_3C		H_3C	85	7.79 ± 3.10

compared to the untreated control cells. The IC values were separately calculated for each experiment and the mean values ± SD were calculated from at least 3–5 independent experiments.

The antiproliferative activities of the bicyclic trioxanes **3a**–**d** against human leukemia (MV4-11) are listed in Table 1. Compounds **3b**–**d** demonstrated a moderate activity (IC_{50} = 7.3–8.0 μM), whereas compound **3a** is inactive (IC_{50} > 39 μM). This suggests that the aromatic group enhances the activity of entries **3b**–**d**.

The cytotoxic activities of the trioxanes derived from the 1,6-dioxabicyclo[4.4.0]-3,9-diene-5-ones **5a**–**w** are summarized in Table 2 against the human leukemia MV4-11 cell line, where the cytotoxic activity of cisplatin is included as a reference compound. All of the compounds in Table 2 are found to be cytotoxic (IC_{50} = 0.549–11.052 μM) against MV4-11, but the 2*H*-pyran, lacking the peroxide ring, exhibits a seven times lower activity (IC_{50} > 24 μM) compared to the average (IC_{50} = 3.6 μM) activity of the trioxane counterparts. This suggests that the peroxide moiety is an important pharmacophore to stop the proliferation of cancer cells.

Compound **5e** shows the lowest cytotoxicity (IC_{50} = 11.052 μM). Compounds **5b**–**d**, **5g**–**h**, **5m**–**r** and **5v** reveal moderate activities (IC_{50} = 3.9–8.5 μM). On the other hand, a very high antiproliferative activity was demonstrated with compounds **5a**, **5f**, **5i**–**l**, **5s**–**u**, and **5w**. Among them, the highest potency is exhibited by compound **5k** (IC_{50} = 0.58 μM), **5l** (IC_{50} = 0.54 μM) and **5s** (IC_{50} = 0.59 μM) with the combination of the substituted aromatic group at C-2 and C-7. Compounds **5k**, **5l** and **5s** show 13 times higher potency compared to its methyl substituted (at C-2) analog, the compound **5b** (IC_{50} = 7.3 μM). Thus, the aromatic group at C-2 might improve the antiproliferative activity. This could be more understandable if we compare the results of entries **5a**–**h** (aliphatic substituent at C-2) and entries **5i**–**w** (aromatic substituent at C-2). However, the anomalous behavior was observed only for compounds **5a** (IC_{50} = 0.98 μM) and **5f** (IC_{50} = 0.89 μM), being 5–10 times more potent than the other compounds with a methyl substituent at C-2.

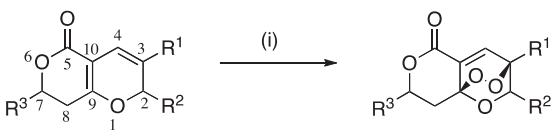

Scheme 2. Synthesis of 7,8-dihydro-2*H*-3,8a-epidioxypyrano[4,3-*b*]pyran-5(3*H*)-one **5**. Reagents and conditions: (i) Rose bengal, O_2, *hν*, MeOH, 0 °C, 1 h.

The diphenyl substituted trioxanes **8a**–**b** show moderate (IC_{50} = 3.0–3.79 μM) and similar antiproliferative activity (Table 3) regardless of kind of the aromatic substituted group at C2 of **8**.

All of the amide derivatives of the trioxanes, **10**, show a good activity with IC_{50} = 0.5–1 μM (Table 4). The combination of the H-acceptor N atom and the aromatic group at C-2 and C-7 is an important feature for the antiproliferative activity in this class of compounds.

The ketone derivatives of the trioxanes, compounds **13c**–**d**, show a low activity, whereas compounds **13a**–**b** are nontoxic to the MV4-11 cell line even though they have an aromatic substituent at C-2 (Table 5). The H-acceptor oxygen atom is important for the better antiproliferative activity.

Accordingly, compounds **5a**, **5f**, **5i**–**l**, **5s**–**u**, **5w** and **10a**–**d** were then chosen for the next study; the antiproliferative activity against human lung (A549) and colon (HCT116) cancer and normal murine fibroblast (BALB/3T3) cell lines. These results are summarized in Table 6. All the tested compounds are cytotoxic against the A549 and HCT116 cell lines, and most of their antiproliferative activities against the cancer cells are similar to that of cisplatin used as the control agent (Table 6). Compound **5j** shows a selectivity among the three cell lines, namely against lung cancer cells A549, it has no cytotoxic effect (IC_{50} > 24 μM), whereas against HCT116 and the normal cell line BALB/3T3, it exhibits a similar activity with the values of IC_{50} = 11.7 and 10.0 μM respectively.

Compounds **5s**–**u** and **10a**–**d** reveal similar activities against the A549 cell line (IC_{50} = 6.2–8.4 μM) compared to the standard cisplatin (IC_{50} = 9.8 μM), but compounds **5a**, **5f**, **5i**–**l** and **5w** display lower activities. Against the colon cancer cell line HCT116, compounds **5a**, **5f** and **5j** show a lower potency than the reference compound (IC_{50} = 8.5 μM). On the other hand, compounds **5i**, **5k**–**l**, **5s**–**5u**, **5w** and **10a**–**d** reveal a slightly higher potency (IC_{50} = 5.5–8.0 μM). The toxicity against the normal mice fibroblast BALB/3T3 by compounds **5a**, **5f**, and **5i**–**l** is lower than that of the reference, cisplatin, however, compounds **5s**–**u**, **5w** and **10a**–**d** are more toxic.

The second stage anticancer screening of compounds **5h**, **5l** and **5o** was performed in order to determine their cytotoxic and growth inhibitory activities across the JFCR39 cancer cell line panel. The compounds were evaluated at five concentration levels (100, 10, 1.0, 0.1, and 0.01 μM). The results (the means of GI50, TGI and LC50 values) are summarized in Table 7.

Table 7 shows that compound **5h** displayed an activity across the JFCR39 panel, HBC-5 (breast cancer) and MKN1 (stomach cancer) being the most sensitive cell lines of the 39 cell lines (GI_{50} = 1.9 μM for both and IC_{50} = 7.7, 6.4 μM, respectively). Compound **5h** also showed a strong antitumor effect on HCT116 (colon, GI_{50} = 2.0 μM, LC_{50} = 17 μM), LOX-IMVI (melanoma, GI_{50} = 2.1 μM,

Table 2
Antiproliferative activity of **5a**–**w** against human leukemia MV4-11 cell line.

Entry	Compound	R^1	R^2	R^3	Yield (%)	MV4-11 IC_{50} (μM)
	Cisplatin					2.820 ± 0.450
1	**5a**			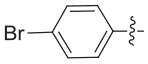	94	0.980 ± 0.155
2	**5b**			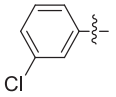	92	7.312 ± 0.774
3	**5c**			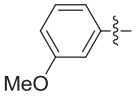	85	7.759 ± 0.031
4	**5d**			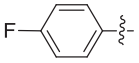	90	6.888 ± 2.100
5	**5e**			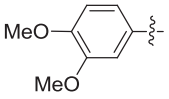	87	11.052 ± 3.904
6	**5f**			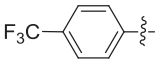	98	0.895 ± 0.465
7	**5g**			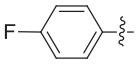	96	8.545 ± 1.203
8	**5h**			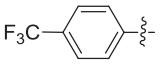	97	5.701 ± 1.020
9	**5i**		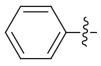	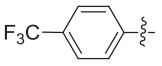	90	0.779 ± 0.129
10	**5j**		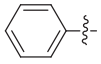	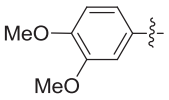	82	0.901 ± 0.275
11	**5k**		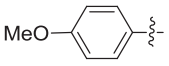	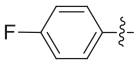	84	0.582 ± 0.100
12	**5l**		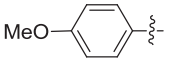	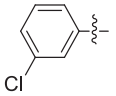	89	0.549 ± 0.175
13	**5m**		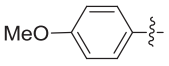	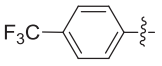	96	4.839 ± 2.071
14	**5n**		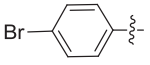	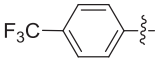	94	5.510 ± 1.307
15	**5o**				88	4.678 ± 1.193
16	**5p**				95	4.314 ± 1.976
17	**5q**				90	4.381 ± 1.748
18	**5r**				92	3.908 ± 1.954

(*continued on next page*)

Table 2 (*continued*)

Entry	Compound	R^1	R^2	R^3	Yield (%)	MV4-11 IC_{50} (μM)
19	**5s**	-CH$_3$	O_2N-	Cl-	93	0.593 ± 0.107
20	**5t**	-CH$_3$	O_2N-	MeO-	87	0.735 ± 0.253
21	**5u**	-CH$_3$	O_2N-	MeO-, MeO	85	0.911 ± 0.331
22	**5v**	-CH$_3$	Br-	Cl-	81	4.205 ± 2.091
23	**5w**	-CH$_3$	O_2N-	Br	85	0.837 ± 0.126
cf	**4m**	-CH$_3$	MeO-	F_3C-		>24

LC_{50} = 8 μM) and OVCAR-3 (ovarian cancer, GI_{50} = 2.1 μM, LC_{50} = 8.1 μM). Compounds **5l** and **5o** were also found to be active against all of the cancer cell lines in the JFCR39 panel. Compound **5l** has a remarkable effect on HBC-5 (breast, GI_{50}: 2.4 μM, LC_{50}: 44 μM) and NCI-H522 (lung cancer, 2.7 μM, LC_{50} = 100 μM). Finally, compound **5o** demonstrated a mentionable potency against LOX-IMVI (melanoma, GI_{50} = 1.0 μM, LC_{50} = 7.5 μM), OVCAR-4 (ovarian, GI_{50} = 1.5 μM, LC_{50} = 42 μM), SK-OV-3 (ovarian, GI_{50} = 1.9 μM, LC_{50} = 58 μM), HBC-5 (breast, GI_{50} = 1.9 μM, LC_{50} = 44 μM) and NCI-H522 (lung cancer, IC_{50} = 2.0 μM, LC_{50} = 22 μM).

3.2. COMPARE study

The COMPARE analysis assesses the correlation coefficient between the *fingerprints* of the test compounds and those of various reference compounds [27]. This system provides an information-intensive approach to identify the molecular targets of new compounds. The JFCR39 COMPARE analysis-guided assay is a successful means to find new anticancer drug candidates. The COMPARE analysis is carried out by calculating the Pearson correlation coefficient (*r* value) between the fingerprints of compounds *X* and *Y*. The *r* value is then used to determine the degree of similarity, that is, the higher the *r* value, the greater the similarity of *X* to *Y*. Generally, an *r* value $0.5 < r < 0.75$ between two agents suggests they might have a similar mechanism of action [28,29] (Fig. 3).

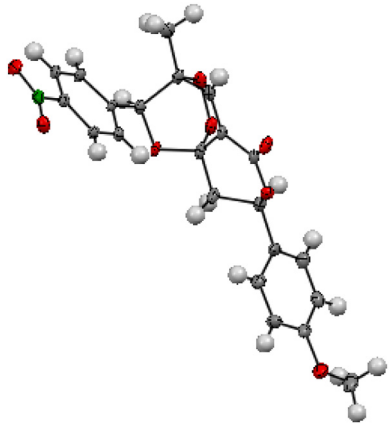

Fig. 2. ORTEP drawing of crystal **5t**.

The COMPARE analysis revealed that compound **5h** has a slight similarity to 6-thioguanine (r = 0.53) and 6-mercaptopurine (r = 0.50). Similarly, compounds **5l** and **5o** have a slight similarity to carmofur (r = 0.49) and 6-thioguanine (r = 0.50), respectively. However, these compounds did not show higher similarity ($r > 0.7$) to reference anticancer drugs, suggesting that they have unique anticancer mechanisms.

3.3. Antimalarial activity

Trioxanes are well-known for their antimalaria activity. The representative trioxanes from the present compound library were tested for the antimalaria activity against the *Plasmodium falciparum* NF54 strain as well as the cytotoxicity against normal cell lines and the data are listed in Table 8. Chloroquine is used as a standard and all of the trioxanes exhibit very weak activity (IC_{50} = 1.08–5.6 μg/mL) compared to the standard. Among the tested trioxanes, mono-substituted (C7) ester compounds **5h**, **5g**, **5l**, **5m** and **10a** show better antimalarial activity (IC_{50} = 1.08–1.97 μg/mL) than their disubstituted (**8a**–**d**) analogs (IC_{50} = 4.20–9.88 μg/mL). Compounds **13b** and **13c** that are the keto derivatives of trioxane show weak potency (IC_{50} = 3.41 and 5.62 μg/mL) against the NF54 strain and against normal cell lines (4.5 and 5.6 μg/mL).

3.4. Docking of heme and endoperoxides

The heme–trioxane interaction plays a key role in generating the reactive oxygen species (ROS), which could cause cellular damage [15]. In order to study the interactions between heme and trioxanes (**5s**), the hemoglobin structure obtained from PDB (1a00) was selected and the heme extracted. Flexible docking was performed by the software, Molecular Operating Environment, (MOE 2011.10) with all the rotational bonds in both trioxanes and heme as variables. The distance between the O^1 and O^4 of the trioxane ring and Fe^{2+} is 1.3, 3 Å respectively, which indicates a definite interaction between heme and the trioxane ring (Fig. 4).

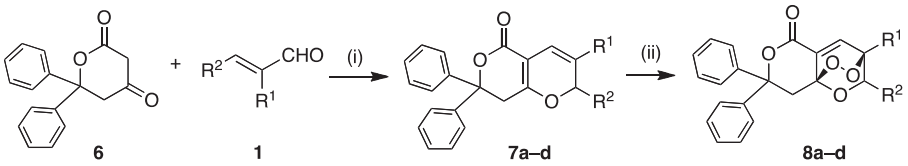

Scheme 3. Synthesis of 7,7-diphenyl-7,8-dihydro-2*H*-3,8a-epidioxypyrano[4,3-*b*]pyran-5(3*H*)-one **8**. Reagents and conditions: (i) ethylenediammonium diacetate (EDDA, 5 mol%), MeOH, 2–3 h, 60 °C. (ii) Rose bengal, O_2, *hν*, MeOH, 0 °C, 1 h.

3.5. Interacting with hemin

The binding study of the compounds **5r**, **5s** and **5u** with hemin was performed using UV–vis absorption spectroscopy in 0.1 M tris buffer (60%, pH 9.0) and DMSO (40%) mixture at ambient temperature. A similar hypochromic effect was observed in other published articles [28,29] while the concentrations of the compounds were increased gradually. Sample concentrations were varied from 0 to 500 μM where the concentration of hemin remains constant (6 μM). Complex formation was monitored after incubation for 12 h and 24 h of the hemin and samples by the decline in absorbance at 402 nm, which essentially remained unchanged. Typical spectral changes observed for the complexation of hemin-endoperoxides are shown below: Figs. 5 and 6.

To study the role of hemin–trioxane interaction in the hemin-induced oxidative damage, methylene blue was selected as a substrate to measure the ability of the heme-catalyzed trioxane oxidizing reaction. The test samples **5r**, **5s** and **5u** were incubated for 2 h at 37 °C with hemin (6 μM) and methylene blue (10 μM) in 0.1 M tris buffer (60%, pH 9.0) and DMSO (40%) mixture. Subsequently, the absorption of the resulting mixture was determined spectrophotometrically [30,31] (Fig. 7).

4. Conclusion

This study described the synthesis of endoperoxides from 1,6-dioxa- or 1-oxa-6-azabicyclo[4.4.0]-3,9-dien-5-ones and 1-oxabi cyclo[4.4.0]-3,9-dien-5-ones and the three-step antiproliferative activities were evaluated. The primary screening was done with 36 candidates against the human leukemia (MV4-11) cancer cell line and 14 of them exhibited a higher potency (IC_{50} = 0.5–1.0 μM) than that of the control cisplatin (IC_{50} = 2.8 μM). The compound without the peroxide ring was also tested and demonstrated more than 50 times less activity than its trioxane congeners, which suggests the important structure activity relationship of the endoperoxides. The most active compounds from the primary screening were chosen for the second step screening against the human lung (A549) and colon cancer (HCT116) and normal murine fibroblast (BALB/3T3) cell lines. Most of them exhibit a better activity than the reference drug cisplatin. Finally, the three candidates were employed for third-step screening against the JFCR39 panel having breast, central nervous system, colon, lung, melanoma, ovarian, renal, stomach and prostate cancer subpanels and 39 cell lines were used to measure the growth factor inhibitory (GI_{50}) and cytotoxicity (IC_{50}). The computer-assisted database analysis, COMPARE suggested that the compounds have unique mechanisms of actions which are different from those of known anticancer drugs. Further modification of the structures and targets is currently underway. The antimalaria activity of the representative trioxanes were examined and revealed very weak potency against the *P. falciparum* NF54 strain. The molecular docking of the representative trioxanes **5s**, **5r** was performed to study the hemin–trioxane interaction. The hemin–trioxane complexation, as well as the role of this interaction in the oxidative damage of methylene blue, was examined for the compounds **5s**, **5r** and **5u** by UV–vis spectroscopy.

Table 3
Antiproliferative activity of **8a**–**d** against human leukemia MV4-11 cell line.

Entry	Compound	R^1	R^2	Yield (%)	MV4-11 IC_{50} (μM)
	Cisplatin				2.820 ± 0.450
1	**8a**	CH_3	O_2N	76	3.79 ± 0.019
2	**8b**	CH_3	MeO	74	3.78 ± 1.092
3	**8c**	CH_3	Cl	92	3.60 ± 0.910
4	**8d**	CH_3	MeOOC	81	2.99 ± 0.281

5. Experimental

5.1. General methods

The commercially obtained reagents were used without further purification. The IR spectra were recorded on a Shimadzu FTIR-8400S spectrometer. The ^{1}H NMR, ^{13}C NMR and ^{19}F NMR spectra were measured on the Varian INOVA-600 or Varian INOVA-400 spectrometer with $CDCl_3$ as a solvent unless otherwise indicated. High resolution mass spectra were obtained on a Bruker micrOTOF II-SKA spectrometer. The UV spectra were recorded with Hitachi U-2910 spectrophotometer in a 1 cm path length quartz cuvette at indicated wavelength, and the sample was dissolved in phosphate buffer with 2.5% DMSO. Melting points were determined on a J-Science RFS-10 hot stage microscope. The scaffolds **3a**–**d**, **4a**–**w**, **6** and **9a**–**d** were prepared by the method we previously reported [24].

5.2. Chemistry

5.2.1. General procedure for the synthesis of *3a–d, 5a–w, 6a–d* and *9a–d*

To a solution of 2*H*-pyrans (1.0 mmol) in MeOH (10 ml), Rose bengal (15 mg) was added and cooled to 0 °C. The reaction flask was fitted with oxygen gas balloon and excited externally with 250 W

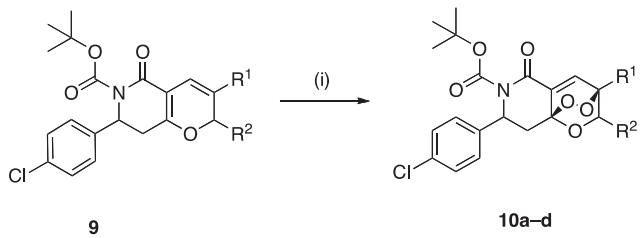

Scheme 4. Synthesis of *N*-protected 5-oxo-2,3,7,8-tetrahydro-3,8a-epidioxypyrano [3,2-*c*]pyridine-6(5*H*)-carboxylate **7**. Reagents and conditions: (i) Rose bengal, O_2, *hν*, MeOH, 0 °C, 1 h.

Table 4
Antiproliferative activity of **10a–d** against human leukemia MV4-11 cell line.

Entry	Compound	R^1	R^2	Yield (%)	MV4-11 IC_{50} (μM)
	Cisplatin				2.820 ± 0.450
1	**10a**	-CH$_3$	O_2N-Ph-	86	0.501 ± 0.062
2	**10b**	-CH$_3$	MeO-Ph-	85	0.661 ± 0.332
3	**10c**	-CH$_3$	-Ph-	87	0.517 ± 0.009
4	**10d**	-CH$_3$	-CH$_3$	84	1.045 ± 0.438

halogen lamps for 1–2 h at 0 °C. The solution was brought to room temperature and solvent was removed in vacuum to afford the crude residue, which was purified by flash column chromatography.

*5.2.2. Methyl 1-ethyl-4-methyl-6-propyl-2,3,5-trioxabicyclo[2.2.2] oct-7-ene-8-carboxylate (**3a**) [24]*

White solids in 85% yield, mp: 137–138 °C (ethyl acetate–hexane); ^{1}H NMR (600 MHz, $CDCl_3$) δ 0.89 (t, J = 7.2 Hz, 3H), 1.03 (m, 1H), 1.04 (t, J = 7.2 Hz, 3H), 1.30 (m, 2H), 1.45 (m, 1H), 1.76 (s, 3H), 1.79 (m, 1H), 1.92 (m, 1H), 3.81 (s, 3H), 4.20 (dd, J = 10.2, 2.4 Hz, 1H), 7.17 (s, 1H); ^{13}C NMR (150.8 MHz, $CDCl_3$) δ 6.8, 13.9, 18.0, 19.6, 24.8, 33.3, 51.9, 76.8, 78.7, 97.0, 136.4, 138.9, 162.5.

*5.2.3. Methyl 1-ethyl-4-phenyl-6-propyl-2,3,5-trioxabicyclo[2.2.2] oct-7-ene-8-carboxylate (**3b**) [24]*

Yield 82%; ^{1}H NMR (600 MHz, $CDCl_3$) δ 0.97 (t, J = 7.2 Hz, 3H), 1.11 (t, J = 7.2 Hz, 3H), 1.19 (m, 1H), 1.44 (m, 2H), 1.62 (m, 1H), 1.88 (m, 1H), 2.00 (m, 1H), 3.54 (s, 3H), 4.41 (d, d, J = 10.8, 2.4 Hz, 1H), 7.23 (s, 1H), 7.39 (m, 3H), 7.54 (m, 2H); ^{13}C NMR (150.8 MHz, $CDCl_3$) δ 6.9, 13.9, 18.1, 24.9, 33.3, 51.9, 77.3, 79.4, 97.4, 126.3 (2C), 127.7 (2C), 129.2, 134.5, 138.36, 138.43, 162.4.

*5.2.4. Methyl 2-methyl-2,5,6,7,8,8a-hexahydro-2,4a-epidioxychromene-3-carboxylate (**3c**) [24]*

Yield 78%; ^{1}H NMR (600 MHz, $CDCl_3$) δ 0.87–1.69 (m, 4H), 1.73 (s) and 1.75 (s) (total 3H), 1.80–2.11 (m, 4H), 3.77 (s) and 3.79 (s) (total 3H), 3.40 and 4.09 (dd, J = 12.0, 5.4 Hz) (total 1H), 7.13 (s) and 7.22 (s) (total 1H); ^{13}C NMR (150.8 MHz, $CDCl_3$) δ 19.5, 19.7, 20.0, 22.5, 22.8, 23.1, 28.4, 29.2, 30.2, 30.3, 51.9, 73.3, 73.7, 75.8, 76.7, 97.1, 98.2, 134.9, 136.1, 139.2, 140.3, 162.4, 162.7.

*5.2.5. Methyl 1,4-dimethyl-6-phenyl-2,3,5-trioxabicyclo[2.2.2]oct-7-ene-8-carboxylate (**3d**) [24]*

Yield 85%; ^{1}H NMR (600 MHz, $CDCl_3$) δ 1.32 (s, 3H), 1.91 (s, 3H), 3.86 (s, 3H), 5.18 (s, 1H), 7.03 (s, 1H), 7.11 (m, 2H), 7.32 (m, 3H); ^{13}C NMR (150.8 MHz, $CDCl_3$) δ 17.8, 19.5, 52.1, 77.1, 80.1, 98.2, 127.4 (2C), 128.3 (2C), 128.7, 136.1, 136.7, 139.7, 162.5.

*5.2.6. 7-(4-Bromophenyl)-2,3-dimethyl-7,8-dihydro-2H-3,8a-epidioxypyrano[4,3-b]pyran-5(3H)-one (**5a**)*

White solids in 94% yield, mp: 169–170 °C (ethyl acetate–hexane); IR (KBr) ν_{max} = 3072, 2982, 2937, 2899, 1732, 1649, 1595, 1491, 1381, 1276, 1188 cm^{-1}; ^{1}H NMR (400 MHz, $CDCl_3$) δ 7.58–7.50 (m, 2H), 7.40–7.35 (m, 1H), 7.33–7.21 (m, 2H), 5.42 (dd, J = 9.0, 5.0 Hz) and 5.32 (dd, J = 12.3, 1.9 Hz) (total 1H), 4.37 (dq, J = 16.3, 6.6 Hz, 1H), 2.50–2.33 (m) and 2.32–2.22 (m) (total 1H), 1.57 (s, 1H) and 1.50 (s, 2H), 1.48–1.41 (m, 1H), 1.03 (dt, J = 6.6, 3.3 Hz, 2H); ^{13}C NMR (101 MHz, $CDCl_3$) δ 140.3 (duplicated), 136.0, 132.0, 131.7 (duplicated), 127.7 (duplicated), 123.0, 95.2, 94.8, 78.5, 78.3, 76.2, 75.4, 36.8, 36.4, 17.3 (duplicated), 16.98. Anal. Calcd for $C_{16}H_{15}BrO_5$: C, 52.34; H, 4.12. Found: C, 52.40; H, 3.92.

*5.2.7. 7-(3-Chlorophenyl)-2,3-dimethyl-7,8-dihydropyrano[4,3-b] pyran-5(2H)-one (**5b**)*

White solids in 92% yield, mp: 152–154 °C (ethyl acetate–hexane); IR (KBr) ν_{max} = 3063, 2978, 2931, 2890, 1728, 1647, 1593, 1438, 1383, 1276, 1190 cm^{-1}; ^{1}H NMR (400 MHz, $CDCl_3$) δ 7.40 (d, J = 9.1 Hz, 2H), 7.37–7.33 (m, 2H), 7.28–7.22 (m, 1H), 5.33 (dd, J = 12.3, 1.8 Hz, 1H), 4.36 (q, J = 6.6 Hz, 1H), 2.45 (dd, J = 15.4, 12.3 Hz, 1H), 2.29 (dd, J = 15.3, 2.0 Hz, 1H), 1.58 (s, 1H), 1.51 (s, 2H), 1.49–1.42 (m, 1H), 1.03 (d, J = 6.6 Hz, 2H); ^{13}C NMR (101 MHz, $CDCl_3$) δ 160.8, 141.9, 140.4, 138.9, 134.8, 131.7, 130.1, 129.1, 126.3, 124.1, 95.1, 78.5, 76.2 (duplicated), 36.8 (duplicated), 17.2 (duplicated), 16.9, 15.0. Anal. Calcd for $C_{16}H_{15}ClO_5$: C, 59.54; H, 4.68. Found: C, 59.12; H, 4.20.

*5.2.8. 7-(3-Methoxyphenyl)-2,3-dimethyl-7,8-dihydro-2H-3,8a-epidioxypyrano[4,3-b]pyran-5(3H)-one (**5c**)*

White solids in 85% yield, mp: 128–129 °C (ethyl acetate–hexane); IR (KBr) ν_{max} = 3074, 2980, 2937, 2835, 1732, 1645, 1600, 1494, 1373, 1274, 1188 cm^{-1}; ^{1}H NMR (400 MHz, $CDCl_3$) δ 7.39 (s, 1H), 7.32 (t, J = 7.9 Hz, 1H), 6.93 (ddd, J = 10.7, 6.6, 4.8 Hz, 3H), 5.34 (dd, J = 12.3, 2.0 Hz, 1H), 4.37 (q, J = 6.7 Hz, 1H), 3.83 (d, J = 1.5 Hz, 3H), 2.49 (dd, J = 15.4, 12.3 Hz) and 2.36–2.26 (m) (total 1H), 1.59 (s) and 1.52 (s) (total 3H), 1.49–1.42 (m) and 1.05 (t, J = 7.3 Hz) (total 3H); ^{13}C NMR (101 MHz, $CDCl_3$) δ 161.2, 159.9, 140.1, 138.4, 131.9, 129.9, 118.2 (duplicated), 114.7, 111.4, 95.3, 78.5, 76.2, 73.8, 55.3, 36.9, 17.3 (duplicated), 16.9. Anal. Calcd for $C_{17}H_{18}O_6$: C, 64.14; H, 5.70. Found: C, 64.24; H, 5.24.

*5.2.9. 7-(4-Fluorophenyl)-2,3-dimethyl-7,8-dihydro-2H-3,8a-epidioxypyrano[4,3-b]pyran-5(3H)-one (**5d**)*

White solids in 90% yield, mp: 145–147 °C (ethyl acetate–hexane); IR (KBr) ν_{max} = 3074, 2985, 2937, 2832, 1736, 1649, 1606, 1516, 1383, 1286, 1188 cm^{-1}; ^{1}H NMR (400 MHz, $CDCl_3$) δ 7.4–7.3 (m, 3H), 7.10 (td, J = 8.6, 1.5 Hz, 2H), 5.44 (dd, J = 8.2, 5.9 Hz) and 5.34 (dd, J = 12.3, 1.8 Hz) (total 1H), 4.37 (dt, J = 19.9, 6.6 Hz, 1H), 2.5–2.3 (m) and 2.27 (ddd, J = 9.4, 2.1, 1.1 Hz) (total 2H), 1.58 (s) and 1.52 (s) (total 3H), 1.40 (m) and 1.04 (t, J = 6.5 Hz) (total 3H); ^{13}C NMR (151 MHz, $CDCl_3$) δ 163.7, 162.1, 161.0, 141.8, 140.3, 140.1, 132.8 (duplicated), 131.82, 128.1–127.9 (m), 115.9, 115.7, 95.2, 94.94 (duplicated), 78.5, 76.30 (duplicated), 75.4, 73.8, 36.8 (duplicated), 36.4, 17.3 (duplicated), 16.9, 15.0. HRMS (FAB) calcd for $[M + H]^+$

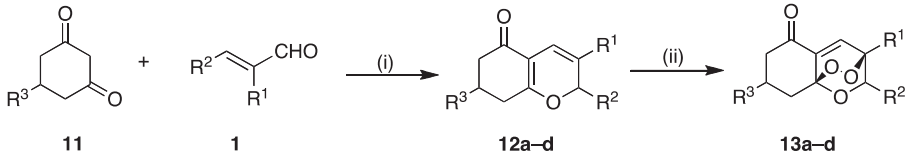

Scheme 5. Synthesis of 2,3,7,8-tetrahydro-3,8a-epidioxychromen-5(6*H*)-one **13**. Reagents and conditions: (i) ethylenediammonium diacetate (EDDA, 5 mol%), MeOH, 2–3 h, 60 °C. (ii) Rose bengal, O_2, *hν*, MeOH, 0 °C, 1 h.

Table 5
Antiproliferative activity of **13a–d** against human leukemia MV4-11 cell line.

Entry	Compound	R^1	R^2	R^3	Yield (%)	MV4-11 IC_{50} (μM)
	Cisplatin					2.820 ± 0.450
1	**13a**		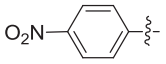	H	96	>31
2	**13b**		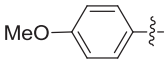	H	97	>33
3	**13c**		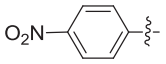	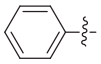	94	6.532 ± 0.660
4	**13d**		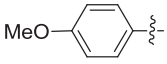	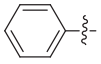	96	6.500 ± 0.951

307.0904. Found 307.0990. Anal. Calcd for $C_{16}H_{15}FO_5$: C, 62.74; H, 4.94. Found: C, 62.46; H, 4.99.

*5.2.10. 7-(3,4-Dimethoxyphenyl)-2,3-dimethyl-7,8-dihydro-2H-3,8a-epidioxypyrano[4,3-b]pyran-5(3H)-one (**5e**)*

White solids in 85% yield, mp: 136–137 °C (ethyl acetate–hexane); IR (KBr) $\nu_{max} = 3068, 2980, 2937, 2837, 1732, 1649, 1595, 1519, 1465, 1271, 1188\ cm^{-1}$; ^1H NMR (300 MHz, $CDCl_3$) δ 7.37 (d, $J = 6.2$ Hz, 1H), 6.99–6.81 (m, 3H), 5.40 (dd, $J = 10.4, 3.5$ Hz) and 5.30 (dd, $J = 12.3, 1.9$ Hz) (total 1H), 4.38 (dd, $J = 11.7, 6.6$ Hz, 1H), 3.99–3.81 (m, 6H), 2.51 (dd, $J = 15.4, 12.3$ Hz) and 2.41–2.21 (m) (total 2H), 1.58 (s) and 1.50 (s) (total 3H), 1.04 (dd, $J = 6.6, 4.8$ Hz, 3H); ^{13}C NMR (101 MHz, $CDCl_3$) δ 161.3, 149.5, 149.2, 140.0 (duplicated), 131.9, 129.3, 118.7 (duplicated), 110.9, 109.1, 95.3, 78.3 (duplicated), 76.2, 75.4, 55.9, 36.7, 36.3, 17.3 (duplicated). Anal. Calcd for $C_{18}H_{20}O_7$: C, 62.06; H, 5.79. Found: C, 62.02; H, 5.51.

*5.2.11. 3-Methyl-2-phenyl-7-(4-(trifluoromethyl)phenyl)-7,8-dihydro-2H-3,8a-epidioxypyrano[4,3-b]pyran-5(3H)-one (**5f**)*

White solids in 86% yield, mp: 173–175 °C (ethyl acetate–hexane); IR (KBr) $\nu_{max} = 3056, 2985, 2941, 2891, 1728, 1653, 1624, 1329, 1276, 1190\ cm^{-1}$; ^1H NMR (300 MHz, $CDCl_3$) δ 7.68 (d, $J = 8.3$ Hz, 2H), 7.57–7.48 (m, 2H), 7.41 (s, 1H), 5.50–5.36 (m, 1H), 4.36 (dd, $J = 6.6, 0.7$ Hz) and 3.77 (d, $J = 6.4$ Hz) (total 1H), 2.55–2.24 (m, 2H), 1.58 (s) and 1.51 (s) (total 3H), 1.4 (d, $J = 6.6$ Hz) and 1.03 (d, $J = 6.6$ Hz) (total 3H); ^{13}C NMR (151 MHz, $CDCl_3$) δ 160.4, 140.9, 140.4, 131.6, 126.31, 125.89 (duplicated), 94.8, 78.3, 76.1, 75.4, 36.5, 17.35 (duplicated). Anal. Calcd for $C_{17}H_{15}F_3O_5$: C, 57.31; H, 4.24. Found: C, 57.14; H, 3.98.

Table 6
Antiproliferative activity of compounds **5a**, **5f**, **5i–l**, **5t–w** and **10a–d** against normal mice fibroblast BALB/3T3 and cancer cell lines A549 and HCT116.

Compound	A549 IC_{50} (μM)	HCT116 IC_{50} (μM)	Balb/3T3 IC_{50} (μM)
Cisplatin	9.870 ± 2.400	8.500 ± 0.540	8.700 ± 0.970
5a	13.017 ± 5.664	9.201 ± 0.811	12.010 ± 2.995
5f	13.92 ± 5.052	9.489 ± 0.785	12.461 ± 1.263
5i	10.92 ± 4.74	7.433 ± 0.341	9.011 ± 0.932
5j	>24	11.744 ± 4.142	10.087 ± 0.779
5k	11.773 ± 4.310	8.082 ± 0.101	9.061 ± 1.681
5l	10.243 ± 3.184	7.665 ± 0.313	8.967 ± 0.819
5s	8.282 ± 0.186	7.37 ± 0.232	8.212 ± 0.162
5t	8.439 ± 0.799	7.496 ± 0.869	7.357 ± 0.658
5u	7.729 ± 1.361	6.785 ± 1.163	7.202 ± 0.812
5w	11.575 ± 0.105	7.084 ± 0.316	7.527 ± 0.210
10a	6.220 ± 0.056	5.539 ± 0.831	6.673 ± 0.529
10b	6.323 ± 0.194	5.562 ± 0.466	6.868 ± 0.544
10c	6.664 ± 0.227	6.023 ± 1.014	5.464 ± 1.262
10d	7.200 ± 0.545	7.300 ± 0.521	6.210 ± 1.896

*5.2.12. 3-(4-Fluorophenyl)-3,4,6,7,8,9-hexahydro-4a,9a-epidioxypyrano[4,3-b]chromen-1(5aH)-one (**5g**)*

White solids in 96% yield, mp: 161–162 °C (ethyl acetate–hexane); IR (KBr) $\nu_{max} = 3076, 2941, 2864, 1732, 1645, 1606, 1514, 1381, 1273, 1226, 1190, 1035\ cm^{-1}$; ^1H NMR (400 MHz, $CDCl_3$) δ 7.49 (d, $J = 5.7$ Hz) and 7.36 (ddd, $J = 7.3, 5.4, 2.6$ Hz) (total 3H), 7.14–7.03 (m, 2H), 5.48–5.39 (m) and 5.39–5.31 (m) (total 1H), 4.22 (td, $J = 12.6, 4.9$ Hz) and 3.57 (ddd, $J = 20.6, 11.2, 5.0$ Hz) (total 1H), 2.45 (td, $J = 15.6, 12.3$ Hz) and 2.32–2.24 (m) (total 2H), 2.24–2.15 (m, 1H), 2.15–2.03 (m, 1H), 2.03–1.70 (m, 3H), 1.70–1.52 (m) and 1.47 (ddd, $J = 13.4, 8.3, 3.5$ Hz) (total 2H), 1.40–1.22 (m, 1H) and 1.00 (ddd, $J = 25.6, 13.0, 3.9$ Hz) (total 1H); ^{13}C NMR (101 MHz, $CDCl_3$) δ 164.1, 161.7, 161.4, 161.1, 141.1, 140.3, 140.0, 132.8, 131.6, 130.5, 128.0 (duplicated), 115.9, 115.7, 96.0, 95.1, 78.4, 78.1, 77.5, 76.3 (duplicated), 75.4, 75.1, 74.2, 36.8 (triply), 30.9, 30.1 (quadruplicated), 29.2 (duplicated), 28.5, 28.2, 23.0–22.5 (m), 22.4, 19.9. Anal. Calcd for $C_{18}H_{17}FO_5$: C, 65.05; H, 5.16. Found: C, 64.91; H, 4.96.

*5.2.13. 3-(4-(Trifluoromethyl)phenyl)-3,4,6,7,8,9-hexahydro-4a,9a-epidioxypyrano[4,3-b]chromen-1(5aH)-one (**5h**)*

White solids in 97% yield, mp: 156–157 °C (ethyl acetate–hexane); IR (KBr) $\nu_{max} = 3068, 2951, 2864, 1735, 1649, 1624, 1431, 1327, 1288, 1174, 1068\ cm^{-1}$; ^1H NMR (400 MHz, $CDCl_3$) δ 7.65 (d, $J = 8.3$ Hz, 2H), 7.53 (d, $J = 8.5$ Hz, 2H), 6.02–5.92 (m, 1H), 5.45 (dd, $J = 12.0, 4.1$ Hz, 1H), 5.05 (ddd, $J = 16.8, 11.4, 5.2$ Hz, 1H), 2.83–2.66 (m, 1H), 2.63–2.47 (m, 1H), 2.40 (dd, $J = 14.1, 1.9$ Hz, 1H), 2.21–2.03 (m, 1H), 2.01–1.87 (m, 2H), 1.85–1.62 (m, 2H), 1.55–1.25 (m, 2H); ^{13}C NMR (101 MHz, $CDCl_3$) δ 164.8 (duplicated), 163.4 (duplicated), 142.3, 131.5 (duplicated), 126.1 (duplicated), 125.6 (quadruplicated), 125.2, 122.5, 109.2, 108.9, 99.6, 99.3, 80.5, 80.3, 75.5 (duplicated), 35.0 (duplicated), 34.0, 33.0, 32.8, 26.8 (duplicated), 24.5 (duplicated). Anal. Calcd for $C_{19}H_{17}F_3O_5$: C, 59.69; H, 4.48. Found: C, 59.76; H, 3.96.

*5.2.14. 3-Methyl-2-phenyl-7-(4-(trifluoromethyl)phenyl)-7,8-dihydro-2H-3,8a-epidioxypyrano[4,3-b]pyran-5(3H)-one (**5i**)*

White solids in 90% yield, mp: 173–175 °C (ethyl acetate–hexane); IR (KBr) $\nu_{max} = 3066, 2991, 2939, 2893, 1732, 1646, 1454, 1329, 1276, 1186\ cm^{-1}$; ^1H NMR (600 MHz, $CDCl_3$) δ 7.70 (d, $J = 8.1$ Hz, 2H), 7.58 (t, $J = 6.4$ Hz, 2H), 7.42–7.29 (m, 4H), 7.15–7.04 (m, 2H), 5.72 (d, $J = 11.3$ Hz) and 5.52 (d, $J = 11.8$ Hz) (total 1H), 5.28 (d, $J = 34.5$ Hz, 1H), 2.63 (dd, $J = 15.5, 12.2$ Hz, 1H), 2.54–2.32 (m, 1H), 1.40 (d, $J = 11.1$ Hz, 3H); ^{13}C NMR (151 MHz, $CDCl_3$) δ 160.5, 141.6, 141.3, 140.8, 134.8, 132.1, 129.2 (duplicated), 128.6 (duplicated),

Table 7
Growth inhibitory (GI_{50}) and cytotoxic (IC_{50}) activities of compounds **5h**, **5l** and **5o** across the JFCR39 panel.

Tissue of origin	Cell line	**5h**			**5l**			**5o**		
		GI_{50} (μM)	TGI (μM)	LC_{50} (μM)	GI_{50} (μM)	TGI (μM)	LC_{50} (μM)	GI_{50} (μM)	TGI (μM)	LC_{50} (μM)
Breast	HBC-4	3.8	14.0	38.0	11	24	54	3.7	13	38
	BSY-1	2.9	8.5	32.0	12	26	57	5.0	17	46
	HBC-5	1.9	3.9	7.7	2.4	8.0	44	1.9	4.1	8.8
	MCF-7	6.4	23	66	11	27	69	10	29	87
	MDA-MB-231	2.9	7.3	27	12	26	58	5.4	18	51
CNS	U251	17	32	64	18	36	73	16	33	68
	SF-268	6.5	25	86	18	41	94	14	36	92
	SF-295	17	33	62	18	33	62	18	33	60
	SF-539	2.3	5.2	28	8.4	23	55	2.8	5.4	14
	SNB-75	11	25	56	12	28	67	12	28	64
	SNB-78	12	31	77	14	34	84	13	34	90
Colon	HCC2998	3.8	17	48	15	30	62	6.3	22	62
	KM-12	12	6.0	58	25	51	100	18	39	85
	HT-29	3.5	15	80	15	48	100	5.2	27	100
	HCT-15	2.6	9.0	50	4.4	24	100	3.7	17	100
	HCT116	2.0	4.9	17	4.1	20	100	3.4	13	70
Lung	NCI-H23	12	31	84	18	40	93	17	36	79
	NCI-H226	20	50	100	20	48	100	18	40	92
	NCI-H522	2.1	5.4	100	2.7	8.6	100	2.0	5.0	22
	NCI-H460	18	38	78	19	38	77	20	41	82
	A549	18	38	83	18	38	78	18	37	72
	DMS273	6.4	22	63	14	31	69	10	27	74
	DMS114	2.3	6.5	27	14	36	92	4.4	20	95
Melanoma	LOX-IMVI	2.1	4.1	8.0	3.1	12	60	1	9	7.5
Ovarian	OVCAR-3	2.1	4.1	8.1	3.4	10	42	2.4	5.1	13
	OVCAR-4	2.3	6.2	31	9.2	24	59	1.5	11	42
	OVCAR-5	2.8	7.6	27	5.3	17	42	2.8	7.4	27
	OVCAR-8	4.8	21	86	12	41	100	9.4	38	100
	SK-OV-3	18	33	58	16	29	54	1.9	33	58
Renal	RXF-631L	17	32	61	16	30	56	17	31	59
	ACHN	14	28	58	16	29	55	15	29	56
Stomach	St-4	18	44	100	19	47	100	18	45	100
	MKN1	1.9	3.5	6.4	4.5	17	49	2.1	4.4	9.1
	MKN7	2.6	7.2	5.5	10	31	97	3.4	14	90
	MKN28	9.3	34	100	14	40	100	11	36	100
	MKN45	15	29	56	14	31	68	16	30	57
	MKN74	9.7	33	100	15	44	100	14	37	96
Prostate	DU145	16	31	58	15	29	54	16	31	57
	PC-3	13	27	56	15	28	55	13	27	56

CNS: central nervous system; GI_{50}: 50% growth inhibition concentration (μM); TGI: total growth inhibition concentration (μM); LC_{50}: lethal concentration (μM).

127.8 (duplicated), 126.3 (duplicated), 125.93 (duplicated), 95.9, 81.8, 80.5, 78.8, 78.6, 76.2 (duplicated), 36.75 (duplicated), 17.68 (duplicated). Anal. Calcd for $C_{22}H_{17}F_3O_5$: C, 63.16; H, 4.10. Found: C, 63.24; H, 3.84.

*5.2.15. 7-(3,4-Dimethoxyphenyl)-3-methyl-2-phenyl-7,8-dihydro-2H-3,8a-epidioxypyrano[4,3-b]pyran-5(3H)-one (**5j**)*

White solids in 82% yield, mp: 155–156 °C (ethyl acetate–hexane); IR (KBr) ν_{max} = 3063, 2941, 2833, 1735, 1647, 1519, 1454, 1267, 1238, 1190, 1026 cm^{-1}, ^1H NMR (400 MHz, $CDCl_3$) δ 7.34 (ddd, J = 21.0, 12.7, 8.4 Hz, 4H), 7.17–7.08 (m, 2H), 7.01–6.93 (m, 2H), 6.88 (d, J = 8.5 Hz, 1H), 5.59 (d, J = 1.6 Hz) and 5.40 (dd, J = 12.2, 1.8 Hz) (total 1H), 5.30 (s) and 5.24 (s) (total 1H), 3.95–3.86 (m, 6H), 2.68 (dd, J = 15.5, 12.3 Hz) and 2.48–2.37 (m) (total 2H), 1.58 (s) and 1.39 (d, J = 8.0 Hz) (total 3H); ^{13}C NMR (101 MHz, $CDCl_3$) δ 160.5, 141.6, 141.3, 134.8, 132.1, 129.2, 128.6 (duplicated), 127.3 (duplicated), 126.3 (duplicated), 125.9 (duplicated), 95.9, 81.8, 80.5, 78.8, 76.2, 36.7, 17.6. Anal. Calcd for $C_{23}H_{22}O_7$: C, 67.31; H, 5.40. Found: C, 67.40; H, 4.95.

*5.2.16. 7-(4-Fluorophenyl)-2-(4-methoxyphenyl)-3-methyl-7,8-dihydro-2H-3,8a-epidioxypyrano[4,3-b]pyran-5(3H)-one (**5k**)*

White solids in 84% yield, mp: 151–152 °C (ethyl acetate–hexane); IR (KBr) ν_{max} = 3076, 2937, 2843, 1722, 1612, 1514, 1383, 1282, 1226, 1195, 1033 cm^{-1}; ^1H NMR (300 MHz, $CDCl_3$) δ 7.47–7.40 (m, 2H), 7.33 (d, J = 10.1 Hz, 1H), 7.16–6.98 (m, 4H), 6.94–6.78 (m, 2H), 5.61 (dd, J = 9.3, 4.7 Hz) and 5.43 (dd, J = 12.2, 1.9 Hz) (total 1H), 5.21 (d, J = 15.7 Hz, 1H), 3.80 (d, J = 3.4 Hz, 3H), 2.63 (dd, J = 15.5, 12.2 Hz) and 2.48–2.32 (m) (total 2H), 1.57 (d, J = 3.2 Hz) and 1.37 (d, J = 5.2 Hz) (total 3H); ^{13}C NMR (101 MHz, $CDCl_3$) δ 164.2, 160.9, 160.2, 141.5, 141.3, 132.7, 132.2, 128.6 (duplicated), 128.0 (duplicated), 127.0 (duplicated), 116.0, 115.8, 114.0 (duplicated), 96.1, 95.6, 81.5, 80.3, 78.8, 76.8–76.2 (m), 55.3 (duplicated), 36.6 (duplicated). Anal. Calcd for $C_{22}H_{19}FO_6$: C, 66.33; H, 4.81. Found: C, 66.25; H, 4.61.

*5.2.17. 7-(3-Chlorophenyl)-2-(4-methoxyphenyl)-3-methyl-7,8-dihydro-2H-3,8a-epidioxypyrano[4,3-b]pyran-5(3H)-one (**5l**)*

White solids in 89% yield, mp: 153–154 °C (ethyl acetate–hexane); IR (KBr) ν_{max} = 3061, 2968, 2841, 1735, 1637, 1612, 1516, 1383, 1283, 1274, 1190, 1074 cm^{-1}; ^1H NMR (400 MHz, $CDCl_3$) δ 7.46 (s, 1H), 7.41–7.32 (m, 4H), 7.10–6.99 (m, 2H), 6.86 (t, J = 9.2 Hz, 2H), 5.60 (dd, J = 11.3, 2.5 Hz) and 5.42 (dd, J = 12.2, 1.9 Hz) (total 1H), 5.21 (d, J = 21.6 Hz, 1H), 3.80 (d, J = 4.4 Hz, 3H), 2.61 (dd, J = 15.5, 12.2 Hz) and 2.51–2.31 (m) (total 2H), 1.58 (s) and 1.37 (d, J = 7.0 Hz) (total 3H); ^{13}C NMR (101 MHz, $CDCl_3$) δ 160.7, 160.2 (duplicated), 141.6, 141.4, 138.8, 134.9, 132.2, 130.2, 129.2, 128.6 (duplicated), 126.9, 126.3 (duplicated), 124.1 (duplicated), 114.0 (duplicated), 96.0, 95.6, 81.5, 80.2, 78.9, 78.7, 76.2 (duplicated), 55.3 (duplicated), 36.7 (duplicated), 17.7 (duplicated). Anal. Calcd for $C_{22}H_{19}ClO_6$: C, 63.70; H, 4.62. Found: C, 63.62; H, 4.40.

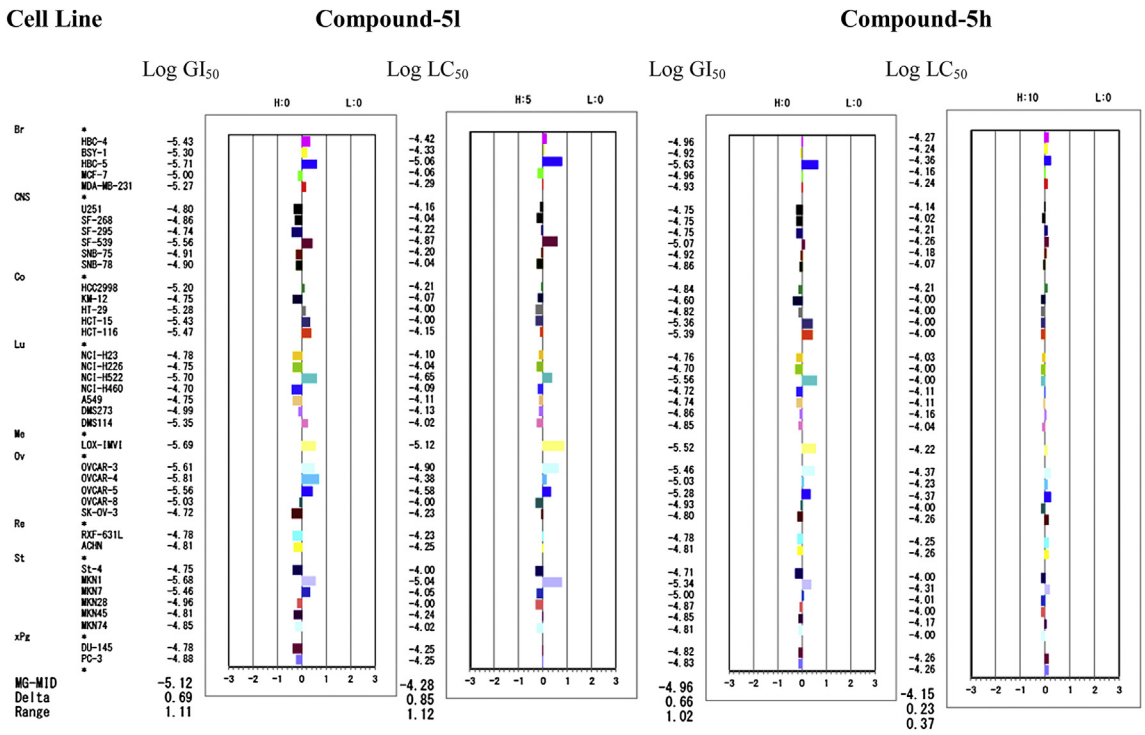

Fig. 3. Growth inhibitory- and cytotoxic activities of compounds **5l** and **5h** across a panel of JFCR39 cell lines. The mean graph was produced by computer processing of the 50% growth inhibition (GI_{50}) and the 50% lethal concentration (LC_{50}) values. Logarithm of the GI_{50} and the LC_{50} values for each cell line are indicated. The *X*-axis shows the difference in logarithmic scale between the mean of Log GI_{50}/Log LC_{50} values for all 39 cell lines (MG-MID, expressed as 0 in the fingerprint) and the Log GI_{50}/Log LC_{50} for each cell line in the JFCR39 panel. Columns to the right of 0 indicate the sensitivity of the cell lines to a given compound and columns to the left indicate their resistance. MG-MID = mean of Log GI_{50}/Log LC_{50} values for all 39 cell lines; delta = difference between the MG-MID and the Log GI_{50}/Log LC_{50} value for the most sensitive cell line; range = difference between the Log GI_{50}/Log LC_{50} values for the most resistant cell line and the most sensitive cell line.

*5.2.18. 2-(4-Methoxyphenyl)-3-methyl-7-(4-(trifluoromethyl) phenyl)-7,8-dihydro-2H-3,8a-epidioxypyrano[4,3-b]pyran-5(3H)-one (**5m**)*

White solids in 96% yield, mp: 158–159 °C (ethyl acetate–hexane); IR (KBr) ν_{max} = 3066, 2939, 2843, 1726, 1647, 1614, 1514, 1327, 1280, 1172, 1124, 1066 cm^{-1}; ^1H NMR (400 MHz, $CDCl_3$) δ 7.70 (d, J = 8.2 Hz, 2H), 7.57 (d, J = 8.2 Hz, 2H), 7.35 (d, J = 11.6 Hz, 1H), 7.03 (tt, J = 9.6, 2.4 Hz, 2H), 6.90–6.80 (m, 2H), 5.69 (dd, J = 11.5, 2.4 Hz) and 5.53–5.48 (m) (total 1H), 5.23 (s) and 5.19 (s) (total 1H), 3.80 (d, J = 5.4 Hz, 3H), 2.61 (dd, J = 15.5, 12.1 Hz) and 2.43 (dddd, J = 18.8, 17.4, 9.5, 7.6 Hz) (total 2H), 1.57 (s) and 1.38 (d, J = 6.6 Hz) (total 3H); ^{13}C NMR (151 MHz, $CDCl_3$) δ 160.6, 160.2, 141.8, 141.6, 140.8, 132.1, 131.3, 128.6 (duplicated), 126.9, 126.36 (duplicated), 125.9 (duplicated), 114.0 (duplicated), 95.9, 95.5, 81.5, 80.3, 78.9, 78.7, 76.22 (duplicated), 55.3 (duplicated), 36.7 (duplicated), 17.6 (duplicated). Anal. Calcd for $C_{23}H_{19}F_3O_6$: C, 61.61; H, 4.27. Found: C, 61.55; H, 3.96.

Table 8
Antimalaria activity of trioxanes against *P. falciparum* NF54 and cytotoxicity against L_6.

Compound	*P. falc.* NF54 IC_{50} μg/mL	Cytotox. L_6 IC_{50} μg/mL
Chloroquine	0.002	0.007
5g	1.17	0.44
5h	1.08	0.50
5j	3.28	0.52
5k	1.68	0.50
5l	1.38	0.46
8a	5.25	3.49
8b	4.20	1.90
8c	9.88	2.03
8d	5.62	1.67
10a	1.97	1.16
13b	3.41	4.5
13c	3.10	5.6

*5.2.19. 2-(4-Bromophenyl)-3-methyl-7-(4-(trifluoromethyl) phenyl)-7,8-dihydro-2H-3,8a-epidioxypyrano[4,3-b]pyran-5(3H)-one (**5n**)*

White solids in 94% yield, mp: 169–171 °C (ethyl acetate–hexane); IR (KBr) ν_{max} = 3070, 2987, 2828, 1720, 1647, 1521, 1383, 1225, 1168, 1066 cm^{-1}; ^1H NMR (400 MHz, $CDCl_3$) δ 7.70 (d, J = 8.2 Hz, 2H), 7.58 (dd, J = 8.2, 2.0 Hz, 2H), 7.53–7.43 (m, 2H), 7.30 (d, J = 10.6 Hz, 1H), 7.04–6.92 (m, 2H), 5.69 (dd, J = 11.5, 2.4 Hz) and 5.51 (dd, J = 12.1, 1.9 Hz) (total 1H), 5.23 (d, J = 21.6 Hz, 1H), 2.62 (dd, J = 15.5, 12.1 Hz) and 2.53–2.36 (m) (total 2H), 1.40 (d, J = 5.4 Hz, 3H); ^{13}C NMR (101 MHz, $CDCl_3$) δ 160.4, 160.1, 141.2, 140.9, 140.7, 134.0 (duplicated), 132.3, 131.8 (duplicated), 128.9 (duplicated), 126.4, 126.1 (duplicated), 125.1, 123.5 (duplicated), 95.9, 95.5, 81.1, 79.9, 78.4 (duplicated), 76.2 (duplicated), 36.6 (duplicated), 29.6, 17.62 (duplicated). Anal. Calcd for $C_{22}H_{16}BrF_3O_5$: C, 53.14; H, 3.24. Found: C, 53.09; H, 3.07.

*5.2.20. 7-(3-Methoxyphenyl)-2-(4-methoxyphenyl)-3-methyl-7,8-dihydro-2H-3,8a-epidioxypyrano[4,3-b]pyran-5(3H)-one (**5o**)*

White solids in 88% yield, mp: 157–158 °C (ethyl acetate–hexane); IR (KBr) ν_{max} = 3063, 2997, 2935, 2839, 1724, 1643, 1612, 1516, 1383, 1278, 1247, 1174, 1028 cm^{-1}; ^1H NMR (400 MHz, $CDCl_3$) δ 7.29–7.36 (m, 3H), 7.06–7.02 (m, 2H), 6.96 (d, J = 13.2, 2H), 6.82–6.92 (m, 2H), 5.57 (q, J = 4.4 Hz) and 5.40 (dd, J = 10.0, 4 Hz) (total

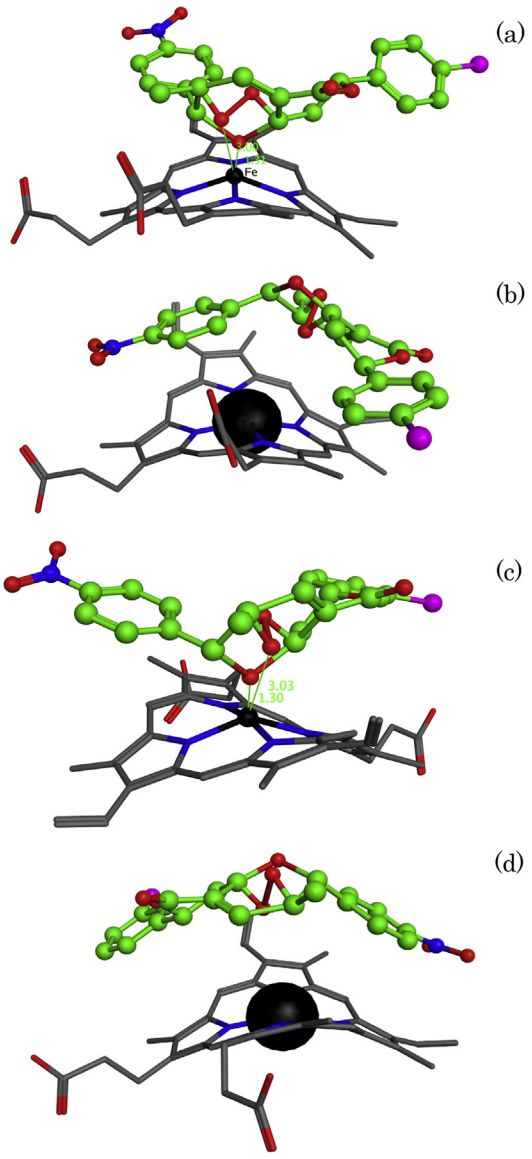

Fig. 4. Molecular docking of trioxane derivatives and heme. (a) and (b) refer to the binding modes of **5s** with heme, the green lines represents the distance of Fe^{2+} (black) to the O^1 (1.31 Å) and O^4 (3 Å) of the trioxane. (c) and (d) represents the binding modes of **5r** with heme, the distances from the green lines represents the distance of Fe^{2+} (black) to the O^1 (1.30 Å) and O^4 (3.03 Å) of the trioxane. (For interpretation of the references to color in this figure legend, the reader is referred to the web version of this article.)

1H), 5.23 (s) and 5.18 (s) (total 1H), 3.81 (t, J = 4 Hz, 6H). 2.63–2.70 (m) and 2.35–2.48 (m) (total 2H), 1.38 (d, J = 8.4 Hz, 3H); ^{13}C NMR (101 MHz, $CDCl_3$) δ 161.2, 160.1, 141.2, 140.9, 132.4, 128.7 (triply), 127.7 (duplicated), 127.1, 114.2, 113.9 (duplicated), 96.2, 95.8, 81.5, 80.2, 78.7 (duplicated), 55.32 (duplicated), 36.4 (duplicated), 17.72 (duplicated). Anal. Calcd for $C_{23}H_{22}O_7$: C, 67.31; H, 5.40. Found: C, 67.15; H, 5.10.

*5.2.21. 7-(4-Chlorophenyl)-2-(4-methoxyphenyl)-3-methyl-7,8-dihydro-2H-3,8a-epidioxypyrano[4,3-b]pyran-5(3H)-one (**5p**)*

White solids in 95% yield, mp: 154–155 °C (ethyl acetate–hexane); IR (KBr) ν_{max} = 3068, 2982, 2935, 2839, 1724, 1647, 1612, 1514, 1381, 1278, 1240, 1182, 1033 cm^{-1}; ^{1}H NMR (400 MHz, $CDCl_3$) δ 7.44–7.30 (m, 5H), 7.08–6.98 (m, 2H), 6.89–6.80 (m, 2H), 5.61 (dd, J = 11.0, 3.1 Hz), 5.43 (dd, J = 12.2, 2.0 Hz) (total 1H), 5.23 (s) and 5.18 (s) (total 1H), 3.80 (d, J = 4.4 Hz, 3H), 2.61 (dd, J = 15.5, 12.2 Hz) and 2.40 (ddd, J = 15.5, 7.1, 2.1 Hz) (total 2H), 1.37 (d, J = 6.9 Hz, 3H); ^{13}C NMR (101 MHz, $CDCl_3$) δ 160.8, 160.2, 141.6, 141.3, 135.4, 135.0, 132.2, 129.1, 128.6 (duplicated), 127.4 (duplicated), 126.9, 114.0 (duplicated), 96.0, 81.5, 80.3, 78.7 (duplicated), 76.37 (duplicated), 55.3, 36.6 (duplicated), 17.7 (duplicated) Anal. Calcd for $C_{22}H_{19}ClO_6$: C, 63.70; H, 4.62. Found: C, 63.57; H, 4.58.

*5.2.22. 7-(3,4-Dimethoxyphenyl)-2-(4-methoxyphenyl)-3-methyl-7,8-dihydro-2H-3,8a-epidioxypyrano[4,3-b]pyran-5(3H)-one (**5q**)*

White solids in 90% yield, mp: 144–145 °C (ethyl acetate–hexane); IR (KBr) ν_{max} = 3068, 2993, 2937, 2837, 1727, 1641, 1612, 1516, 1448, 1381, 1261, 1238, 1184, 1026 cm^{-1}; ^{1}H NMR (400 MHz, $CDCl_3$) δ 7.34 (s) and 7.31 (s) (total 1H), 7.05 (dd, J = 8.6, 6.3 Hz, 2H), 7.00–6.92 (m, 2H), 6.91–6.81 (m, 3H), 5.57 (s) and 5.39 (dd, J = 12.2, 1.8 Hz) (total 1H), 5.24 (s) and 5.18 (s) (total 1H), 3.96–3.86 (m, 6H), 3.84–3.76 (m, 3H), 2.67 (dd, J = 15.5, 12.3 Hz, 1H), 2.48–2.35 (m, 1H), 1.37 (d, J = 7.1 Hz, 3H); ^{13}C NMR (101 MHz, $CDCl_3$) δ 161.2, 160.1, 149.6, 149.2, 141.3, 141.0, 132.4, 129.2, 128.6 (duplicated), 127.1 (duplicated), 118.7 (duplicated), 113.9 (duplicated), 111.0, 109.1 (duplicated), 96.2, 81.5, 80.2, 78.7 (duplicated), 55.9 (duplicated), 55.3 (duplicated), 36.6 (duplicated), 17.7 (duplicated). Anal. Calcd for $C_{24}H_{24}O_8$: C, 65.45; H, 5.49. Found: C, 65.30; H, 5.35.

*5.2.23. 7-(3-Chlorophenyl)-3-methyl-2-(4-nitrophenyl)-7,8-dihydro-2H-3,8a-epidioxypyrano[4,3-b]pyran-5(3H)-one (**5r**)*

White solids in 90% yield, mp: 167–168 °C (ethyl acetate–hexane); IR (KBr) ν_{max} = 3080, 2985, 2860, 1732, 1608, 1521, 1350, 1276, 1192, 1035 cm^{-1}; ^{1}H NMR (400 MHz, $CDCl_3$) δ 8.22 (d, J = 8.7 Hz, 1H), 8.16 (d, J = 8.7 Hz, 1H), 7.47 (d, J = 1.2 Hz, 1H), 7.42–7.21 (m, 6H), 5.63 (dd, J = 11.1, 2.8 Hz), 5.48–5.39 (m) and 5.36 (s) (total 2H), 2.68 (dd, J = 15.5, 12.1 Hz) and 2.54–2.38 (m) (total 2H), 1.43 (d, J = 3.4 Hz, 3H); ^{13}C NMR (101 MHz, $CDCl_3$) δ 160.2, 159.9, 148.3, 141.9 (duplicated), 140.2 (duplicated), 138.5 (duplicated), 134.9, 132.5, 130.2 (duplicated), 129.3 (duplicated), 128.3 (duplicated), 126.2 (duplicated), 124.2, 124.0, 123.7 (duplicated), 95.9, 95.5, 80.6, 79.5, 78.2 (duplicated), 76.2, 36.3 (duplicated), 17.6 (duplicated). Anal. Calcd for $C_{21}H_{16}ClNO_7$: C, 58.68; H, 3.75; N, 3.26. Found: C, 58.55; H, 3.63; N, 3.16.

*5.2.24. 7-(4-Chlorophenyl)-3-methyl-2-(4-nitrophenyl)-7,8-dihydro-2H-3,8a-epidioxypyrano[4,3-b]pyran-5(3H)-one (**5s**)*

White solids in 93% yield, mp: 180–181 °C (ethyl acetate–hexane); IR (KBr) ν_{max} = 3072, 2987, 2939, 1732, 1606, 1523, 1350, 1276, 1192, 1014 cm^{-1}; ^{1}H NMR (300 MHz, $CDCl_3$) δ 8.27–8.15 (m, 2H), 7.46–7.22 (m, 7H), 5.63 (dd, J = 10.4, 3.6 Hz) and 5.48–5.39 (m) and 5.36 (s) (total 2H), 2.65 (dd, J = 15.5, 12.0 Hz) and 2.56–2.34 (m) (total 2H), 1.43 (d, J = 4.0 Hz, 3H); ^{13}C NMR (101 MHz, $CDCl_3$) δ 160.0, 148.4, 141.9 (duplicated), 140.2 (duplicated), 135.1 (duplicated), 132.5, 129.2 (duplicated), 128.3 (duplicated), 127.4 (duplicated), 123.7 (duplicated), 95.61, 80.7, 79.5, 78.2 (duplicated), 76.4, 36.4 (duplicated), 17.6 (duplicated). Anal. Calcd for $C_{21}H_{16}ClNO_7$: C, 58.68; H, 3.75; N, 3.26. Found: C, 58.68; H, 3.38; N, 3.13.

*5.2.25. 7-(4-Methoxyphenyl)-3-methyl-2-(4-nitrophenyl)-7,8-dihydro-2H-3,8a-epidioxypyrano[4,3-b]pyran-5(3H)-one (**5t**)*

White solids in 87% yield, mp: 177–178 °C (ethyl acetate–hexane); IR (KBr) ν_{max} = 3080, 2937, 2839, 1728, 1612, 1519, 1350, 1251, 1180, 1033 cm^{-1}; ^{1}H NMR (300 MHz, $CDCl_3$) δ 8.21 (ddt, J = 11.1, 9.2, 2.1 Hz, 2H), 7.40–7.19 (m, 5H), 6.99–6.90 (m, 2H), 5.60 (dd, J = 9.2, 4.9 Hz) and 5.42 (dd, J = 11.6, 2.4 Hz) and 5.36 (s) (total 2H), 3.83 (s, 3H), 2.71 (dd, J = 15.5, 12.0 Hz) and 2.53–2.36 (m) (total 2H), 1.43 (d, J = 4.9 Hz, 3H); ^{13}C NMR (101 MHz, $CDCl_3$) δ 160.7, 160.2, 148.3, 141.9, 139.8, 132.8, 128.5 (duplicated), 127.7, 123.7 (duplicated),

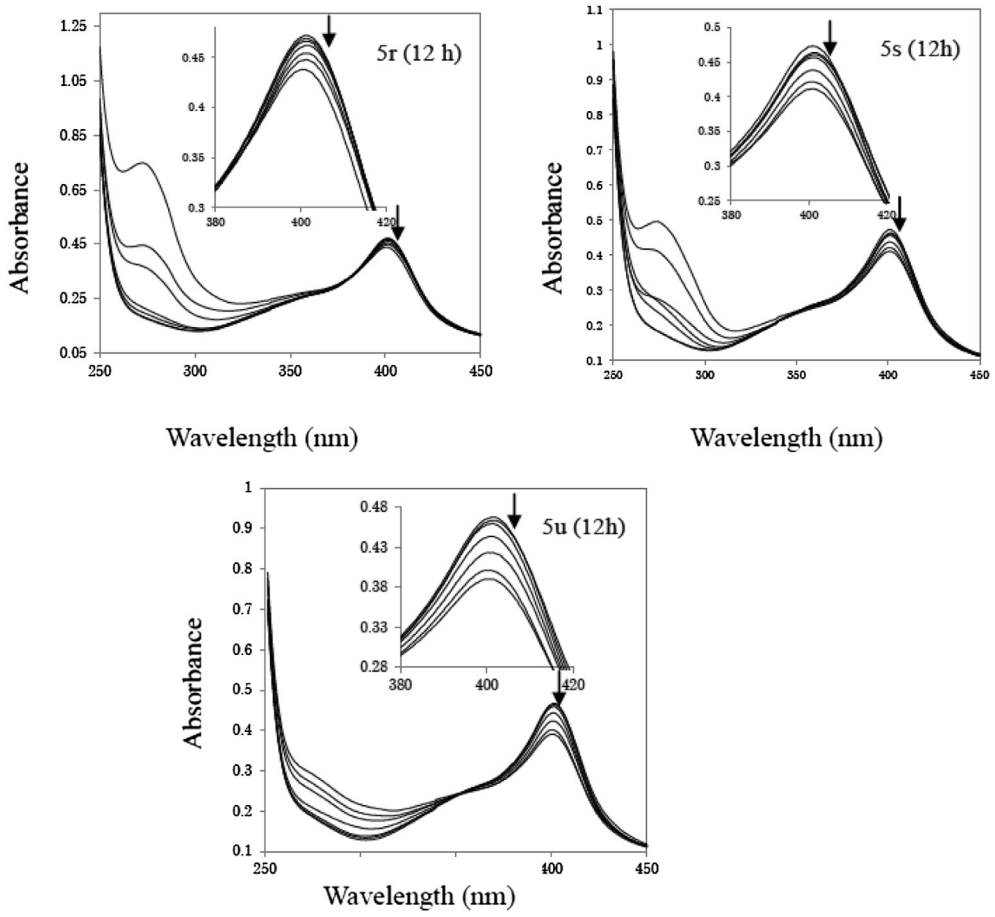

Fig. 5. UV–vis absorption spectra of the compounds **5r**, **5s** and **5u** after the incubation for 12 h at 37 °C in 0.1 M tris buffer (60%, pH 9.0) and DMSO (40%) mixture. The curves 1–7 for the C_{hemin} = 6 μM and $C_{\mathbf{5r},\ \mathbf{5s},\ \mathbf{5u}}$ = 0, 25, 50, 150, 300, 400 and 500 μM to the final solution. A gradual hypochromic shift of the absorptions is observed as the compounds concentrations are increases.

114.2, 96.1, 80.6, 78.2, 55.39, 36.2, 17.6. Anal. Calcd for $C_{22}H_{19}NO_8$: C, 62.12; H, 4.50; N, 3.29. Found: C, 62.33; H, 4.42; N, 3.19.

*5.2.26. 7-(3,4-Dimethoxyphenyl)-3-methyl-2-(4-nitrophenyl)-7,8-dihydro-2H-3,8a-epidioxypyrano[4,3-b]pyran-5(3H)-one (**5u**)*

White solids in 85% yield, mp: 174–175 °C (ethyl acetate–hexane); IR (KBr) ν_{max} = 3076, 2939, 2835, 1730, 1608, 1523, 1352, 1274, 1190, 1024 cm^{-1}; ^1H NMR (300 MHz, $CDCl_3$) δ 8.29–8.12 (m, 2H), 7.30 (dt, J = 17.6, 8.5 Hz, 3H), 7.02–6.84 (m, 3H), 5.59 (dd, J = 8.7, 5.4 Hz) and 5.45–5.32 (m) (total 2H), 3.91 (d, J = 4.8 Hz, 6H), 2.70 (dd, J = 15.5, 12.1 Hz) and 2.54–2.37 (m) (total 2H), 1.43 (d, J = 4.5 Hz, 3H); ^{13}C NMR (101 MHz, $CDCl_3$) δ 160.7, 149.7, 149.3, 148.3, 142.2 (duplicated), 139.9, 132.7, 128.9, 128.4, 123.7 (duplicated), 118.7 (duplicated), 111.0, 109.1, 96.1, 95.7, 80.6, 78.1 (duplicated), 55.9, 36.4, 17.6. Anal. Calcd for $C_{23}H_{21}NO_9$: C, 60.66; H, 4.65; N, 3.08. Found: C, 60.75; H, 4.53; N, 3.05.

*5.2.27. 2-(4-Bromophenyl)-7-(4-chlorophenyl)-3-methyl-7,8-dihydro-2H-3,8a-epidioxypyrano[4,3-b]pyran-5(3H)-one (**5v**)*

White solids in 81% yield, mp: 178–179 °C (ethyl acetate–hexane); IR (KBr) ν_{max} = 3070, 2987, 2901, 1720, 1647, 1494, 1383, 1282, 1197, 1070 cm^{-1}; ^1H NMR (300 MHz, $CDCl_3$) δ 7.49–7.29 (m, 6H), 7.28–7.20 (m, 1H), 7.00–6.90 (m, 2H), 5.56 (s) and 5.39 (dd, J = 12.1, 2.1 Hz) (total 1H), 5.19 (d, J = 15.5 Hz, 1H), 2.58 (dd, J = 15.5, 12.1 Hz) and 2.43–2.28 (m) (total 2H), 1.35 (d, J = 4.4 Hz, 3H); ^{13}C NMR (101 MHz, $CDCl_3$) δ 160.6, 140.9, 140.7, 135.2, 135.0, 134.0 (duplicated), 132.3, 131.82 (duplicated), 129.2–128.5 (m), 127.4 (duplicated), 123.4, 95.9, 95.5, 81.1, 79.9, 78.4 (duplicated), 76.3 (duplicated), 36.5 (duplicated), 17.6 (duplicated). Anal. Calcd for $C_{21}H_{16}BrClO_5$: C, 54.39; H, 3.48. Found: C, 54.47; H, 3.34.

*5.2.28. 7-(3-Bromophenyl)-3-methyl-2-(4-nitrophenyl)-7,8-dihydro-2H-3,8a-epidioxypyrano[4,3-b]pyran-5(3H)-one (**5w**)*

White solids in 84% yield, mp: 164–165 °C (ethyl acetate–hexane); IR (KBr) ν_{max} = 3080, 2985, 2937, 1732, 1651, 1606, 1521, 1350, 1276, 1192, 1035 cm^{-1}; ^1H NMR (400 MHz, $CDCl_3$) δ 8.30–8.19 (m, 1H), 8.19–8.08 (m, 1H), 7.63 (dd, J = 3.8, 1.8 Hz, 1H), 7.57–7.47 (m, 1H), 7.44–7.17 (m, 5H), 5.62 (dd, J = 11.2, 2.7 Hz) and 5.50–5.30 (m) (total 2H), 2.67 (dd, J = 15.5, 12.1 Hz) and 2.57–2.36 (m) (total 2H), 1.44 (d, J = 4.0 Hz, 3H); ^{13}C NMR (101 MHz, $CDCl_3$) δ 160.2, 148.3, 141.9 (duplicated), 140.2 (duplicated), 138.8, 132.5 (triply), 130.5, 129.1 (duplicated), 128.3 (duplicated), 124.7, 124.5, 123.7 (duplicated), 123.0, 95.9, 95.5, 80.6, 79.5, 78.2 (duplicated), 76.1, 36.4 (duplicated), 17.62 (duplicated). Anal. Calcd for $C_{21}H_{16}BrNO_7$: C, 53.18; H, 3.40; N, 2.95. Found: C, 53.03; H, 3.19; N, 2.76.

*5.2.29. 3-Methyl-2-(4-nitrophenyl)-7,7-diphenyl-7,8-dihydro-2H-3,8a-epidioxypyrano[4,3-b]pyran-5(3H)-one (**8a**)*

White solids in 76% yield, mp: 202–203 °C (ethyl acetate–hexane); IR (KBr) ν_{max} = 3070, 2993, 2931, 1724, 1643, 1521, 1450, 1346, 1267 cm^{-1}; ^1H NMR (400 MHz, $CDCl_3$) δ 7.86 (d, J = 8.8 Hz, 2H), 7.60 (dd, J = 7.5, 2.2 Hz, 2H), 7.45–7.28 (m, 8H), 7.07 (s, 1H), 6.35 (d,

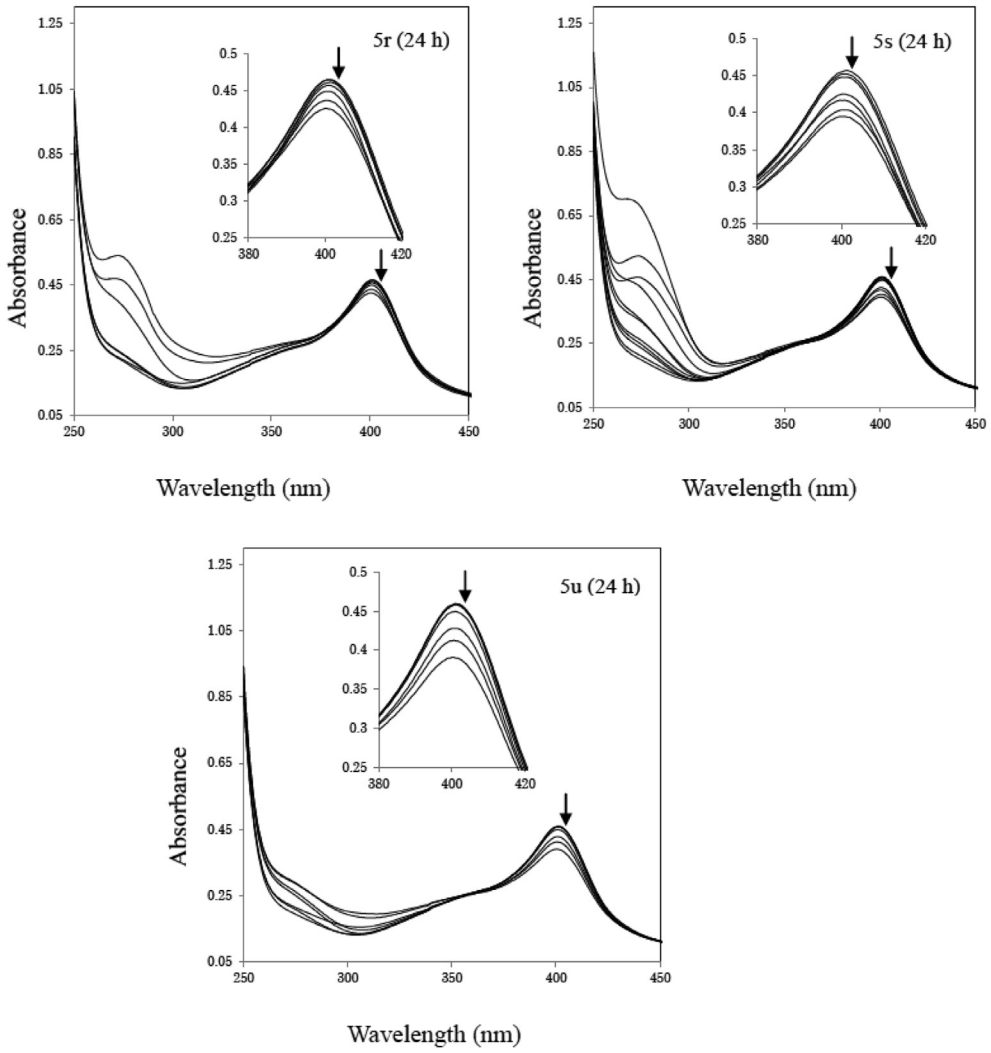

Fig. 6. UV–vis absorption spectra of the mixture of hemin and compounds **5r**, **5s** and **5u** after the incubation for 24 h at 37 °C in 0.1 M tris buffer (60%, pH 9.0) and DMSO (40%) mixture. The curves 1–7 are for the $C_{hemin} = 6$ μM and $C_{\mathbf{5r},\ \mathbf{5s},\ \mathbf{5u}} = 0$, 25, 50, 150, 300, 400 and 500 μM to the final solution. A gradual hypochromic shift of the absorptions at 402 nm is observed as the compounds concentrations are increases.

$J = 8.5$ Hz, 2H), 5.24 (s, 1H), 3.40 (dd, $J = 15.4$, 0.5 Hz, 1H), 2.93 (d, $J = 15.5$ Hz, 1H), 1.35 (s, 3H); ^{13}C NMR (101 MHz, $CDCl_3$) δ 160.3, 142.4, 141.9, 141.2, 139.7, 131.7, 128.5 (duplicated), 127.9, 127.1, 125.4, 123.2, 95.43, 85.94, 80.17, 78.21, 38.2, 17.6; Anal. Calcd for $C_{27}H_{21}NO_7$: C, 68.78; H, 4.49; N, 2.97. Found: C, 68.81; H, 4.55; N, 2.88.

*5.2.30. 2-(4-Methoxyphenyl)-3-methyl-7,7-diphenyl-7,8-dihydro-2H-3,8a-epidioxypyrano[4,3-b]pyran-5(3H)-one (**8b**)*

White solids in 82% yield, mp: 175–176 °C (ethyl acetate–hexane); IR (KBr) $\nu_{max} = 3055$, 2999, 2837, 1739, 1645, 1514, 1388, 1271, 1174 cm^{-1}; ^{1}H NMR (600 MHz, $CDCl_3$) δ 7.36 (dd, $J = 8.3$, 1.0 Hz, 2H), 7.30 (t, $J = 7.7$ Hz, 2H), 7.27–7.11 (m, 8H), 6.87–6.78 (m, 2H), 6.23 (s, 1H), 5.64 (s, 1H), 3.84 (s, 3H), 3.23 (d, $J = 17.6$ Hz, 1H), 3.12 (d, $J = 17.6$ Hz, 1H), 1.56 (d, $J = 7.8$ Hz, 3H); ^{13}C NMR (151 MHz, $CDCl_3$) δ 164.5, 161.9, 160.2, 143.4, 142.5, 130.1, 129.3, 128.43 (duplicated), 127.66 (duplicated), 125.8, 125.4, 125.1, 114.1, 113.2, 102.0, 83.9, 82.93, 55.3, 37.3, 19.2; Anal. Calcd for $C_{28}H_{24}O_6$: C, 73.67; H, N, 5.30. Found: C, 73.79; H, 5.31.

*5.2.31. 2-(4-Chlorophenyl)-3-methyl-7,7-diphenyl-7,8-dihydro-2H-3,8a-epidioxypyrano[4,3-b]pyran-5(3H)-one (**8c**)*

White solids in 88% yield, mp: 180–181 °C (ethyl acetate–hexane); IR (KBr) $\nu_{max} = 3063$, 3005, 2955, 1724, 1645, 1448, 1348, 1280, 1182 cm^{-1}; ^{1}H NMR (600 MHz, $CDCl_3$) δ 7.59–7.55 (m, 2H), 7.41 (dd, $J = 8.4$, 1.0 Hz, 2H), 7.39–7.31 (m, 5H), 7.29 (d, $J = 7.3$ Hz, 1H), 7.09 (s, 1H), 7.01–6.97 (m, 2H), 6.16 (d, $J = 8.4$ Hz, 2H), 5.10 (s, 1H), 3.37 (d, $J = 15.5$ Hz, 1H), 2.91 (d, $J = 15.5$ Hz, 1H), 1.31 (s, 3H); ^{13}C NMR (151 MHz, $CDCl_3$) δ 160.6, 142.6, 141.2, 140.4, 134.48, 133.4, 131.4, 128.6, 128.3, 127.0, 125.4, 95.4, 85.9, 80.4, 78.4, 38.41 (s, 5H), 31.5, 22.6, 17.6, 14.1. Anal. Calcd for $C_{27}H_{21}ClO_5$: C, 70.36; H, 4.59. Found: C, 70.78; H, 5.22.

*5.2.32. Methyl 4-(3-methyl-5-oxo-7,7-diphenyl-3,5,7,8-tetrahydro-2H-3,8a-epidioxypyrano[4,3-b]pyran-2-yl)benzoate (**8d**)*

White solids in 76% yield, mp: 200–201 °C (ethyl acetate–hexane); IR (KBr) $\nu_{max} = 3063$, 2955, 1722, 1651, 1492, 1450, 1348, 1197 cm^{-1}; ^{1}H NMR (600 MHz, $CDCl_3$) δ 7.68 (d, $J = 8.4$ Hz, 2H), 7.60–7.55 (m, 2H), 7.43–7.40 (m, 2H), 7.40–7.31 (m, 5H), 7.29 (d, $J = 7.3$ Hz, 1H), 7.08 (s, 1H), 6.30 (d, $J = 8.2$ Hz, 2H), 5.19 (s, 1H), 3.90 (s, 3H), 3.38 (d, $J = 15.4$ Hz, 1H), 2.93 (d, $J = 15.4$ Hz, 1H), 1.31 (s, 3H); ^{13}C NMR (151 MHz, $CDCl_3$) δ 166.4, 160.6, 142.6, 141.2, 140.3, 139.8, 131.5, 130.3, 129.2, 128.64 (duplicated), 128.4, 128.2, 127.03 (duplicated), 125.4, 95.4, 85.9, 80.7, 78.4, 52.2, 38.4, 17.6; Anal. Calcd for $C_{29}H_{24}O_7$: C, 71.89; H, 4.99. Found: C, 71.20; H, 4.56.

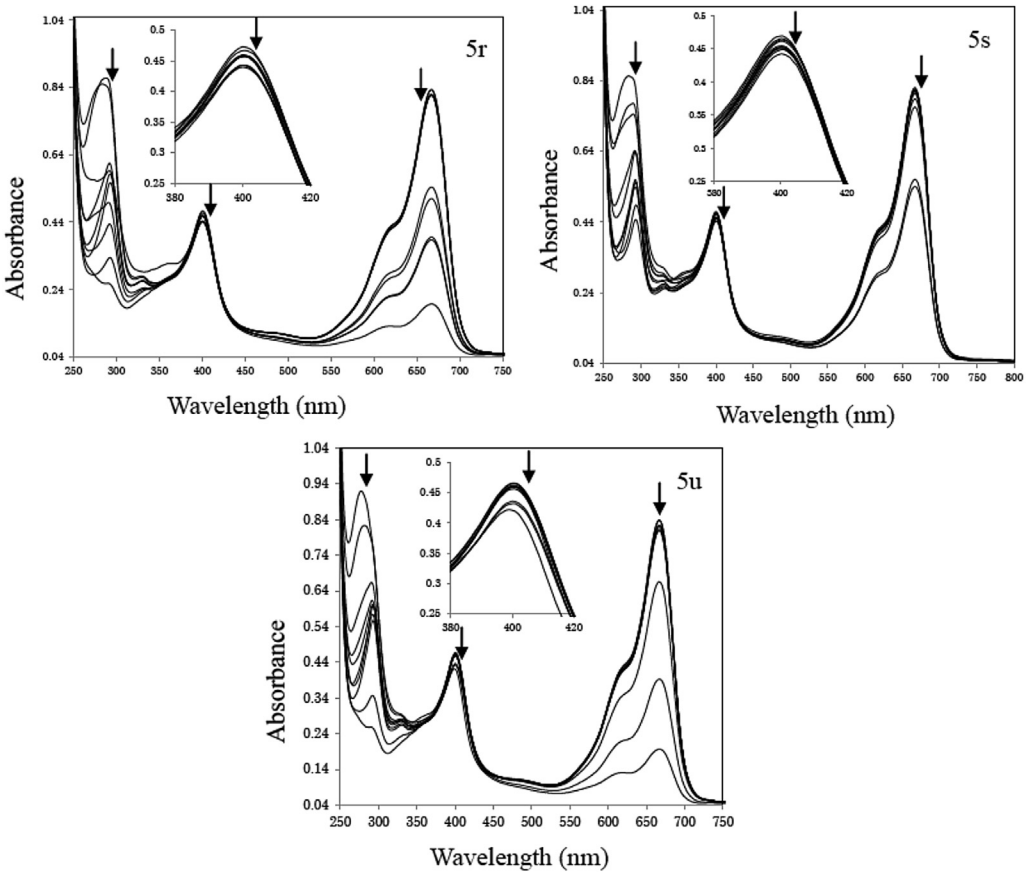

Fig. 7. UV–vis absorption spectra of the mixture of hemin, methylene blue and compounds **5r**, **5s** and **5u** after the incubation for 2 h at 37 °C in 0.1 M tris buffer (60%, pH 9.0) and DMSO (40%) mixture. The curves 1–10 are for the C_{hemin} = 6 μM, $C_{M.\ blue}$ = 10 μM, $C_{\mathbf{5r},\ \mathbf{5s},\ \mathbf{5u}}$ = 0, 5, 10, 25, 50, 100, 200, 300, 500 and 700 μM to the final solution. A regular hypochromic shift of the absorptions at 400 nm is observed for hemin and at 290 and 668 nm for methylene blue as the compounds concentrations are increases.

*5.2.33. tert-Butyl 7-(4-chlorophenyl)-3-methyl-2-(4-nitrophenyl)-5-oxo-2,3,7,8-tetrahydro-3,8a-epidioxypyrano[3,2-c]pyridine-6(5H)-carboxylate (**10a**)*

White solids in 86% yield, mp: 163–164 °C (ethyl acetate–hexane); IR (KBr) ν_{max} = 3084, 2983, 2927, 1776, 1720, 1645, 1521, 1384, 1288, 1149 cm^{-1}; ^1H NMR (600 MHz, $CDCl_3$) δ 7.95 (d, J = 8.6 Hz, 2H), 7.37 (d, J = 8.5 Hz, 2H), 7.27 (d, J = 8.0 Hz, 2H), 7.06 (s, 1H), 6.49 (d, J = 8.6 Hz, 2H), 5.73 (s, 1H), 5.16 (s, 1H), 2.89 (dd, J = 15.0, 4.2 Hz, 1H), 2.62 (dd, J = 15.0, 4.9 Hz, 1H), 1.51 (d, J = 12.6 Hz, 9H), 1.35 (s, 3H); ^{13}C NMR (151 MHz, $CDCl_3$) δ 159.2, 151.8, 147.9, 142.1, 138.3, 137.9, 137.5, 135.7, 133.6, 128.9, 128.8, 128.4, 127.7 (duplicated), 126.7, 123.6, 123.1, 95.7 (duplicated), 84.8, 80.1, 79.8, 78.2, 60.3, 55.1, 54.4, 35.6, 34.2, 27.8, 17.6, 17.49, 14.1. Anal. Calcd for $C_{26}H_{25}ClN_2O_8$: C, 59.04; H, 4.76; N, 5.30. Found: C, 58.96; H, 4.59; N, 5.23.

*5.2.34. tert-Butyl 7-(4-chlorophenyl)-2-(4-methoxyphenyl)-3-methyl-5-oxo-2,3,7,8-tetrahydro-3,8a-epidioxypyrano[3,2-c] pyridine-6(5H)-carboxylate (**10b**)*

White solids in 87% yield, mp: 157–158 °C (ethyl acetate–hexane); IR (KBr) ν_{max} = 3060, 2983, 2883, 1770, 1716, 1639, 1492, 1369, 1294, 1153, 1012 cm^{-1}; ^1H NMR (600 MHz, $CDCl_3$) δ 7.35–7.31 (m, 2H), 7.31–7.27 (m, 1H), 7.25 (d, J = 9.0 Hz, 2H), 7.13 (s, 1H), 7.06 (d, J = 8.5 Hz) and 7.01 (d, J = 8.7 Hz) (total 1H), 6.61 (d, J = 8.7 Hz, 1H), 6.28 (d, J = 8.7 Hz, 1H), 5.66 (t, J = 4.6 Hz) and 5.61 (dd, J = 9.5, 5.6 Hz) (total 1H), 5.01 (d, J = 9.3 Hz, 1H), 3.75 (s, 3H), 2.84 (dd, J = 15.0, 4.6 Hz, 1H), 2.57 (dd, J = 15.0, 4.9 Hz, 1H), 1.54–1.43 (m, 9H), 1.30 (s, 3H); ^{13}C NMR (151 MHz, $CDCl_3$) δ 160.0, 159.7 (duplicated), 151.9, 151.6, 139.6, 139.1, 138.1, 137.6, 135.3, 133.7, 128.9–128.6 (m), 128.2, 127.7, 127.4, 127.1, 126.8, 113.8, 113.3, 95.9 (duplicated), 84.5 (duplicated), 81.0, 80.5, 78.9, 55.2 (duplicated), 54.7–54.5 (m), 34.6, 27.8, 17.7. Anal. Calcd for $C_{27}H_{28}ClNO_7$: C, 63.10; H, 5.49; N, 2.73. Found: C, 63.05; H, 5.28; N, 2.83.

*5.2.35. tert-Butyl 7-(4-chlorophenyl)-3-methyl-5-oxo-2-phenyl-2,3,7,8-tetrahydro-3,8a-epidioxypyrano[3,2-c]pyridine-6(5H)-carboxylate (**10c**)*

White solids in 87% yield, mp: 109–110 °C (ethyl acetate–hexane); IR (KBr) ν_{max} = 3071, 2982, 2935, 2839, 1770, 1722, 1639, 1514, 1359, 1288, 1151, 1001 cm^{-1}; ^1H NMR (400 MHz, $CDCl_3$) δ 7.38–7.16 (m, 6H), 7.09 (ddd, J = 11.0, 6.5, 5.2 Hz, 3H), 6.42–6.36 (m, 1H), 5.66 (t, J = 4.7 Hz, 1H), 5.07 (d, J = 4.5 Hz, 1H), 2.94–2.78 (m, 1H), 2.59 (dd, J = 15.0, 4.9 Hz, 1H), 1.59 (s) and 1.49 (d, J = 2.9 Hz) (total 9H), 1.32 (s) and 1.26 (s) (total 3H); ^{13}C NMR (101 MHz, $CDCl_3$) δ 159.7, 151.9, 139.5, 138.9, 137.6, 135.9, 135.0, 133.1, 129.1–128.4 (m), 127.9, 127.6 (duplicated), 126.91 (duplicated), 95.9, 84.5 (duplicated), 81.3, 80.8, 78.8, 78.3, 55.3, 54.7, 35.7, 34.6, 27.8 (duplicated), 17.6 (duplicated). Anal. Calcd for $C_{26}H_{26}ClNO_6$: C, 64.53; H, 5.42; N, 2.89. Found: C, 64.49; H, 5.38; N, 2.61.

*5.2.36. tert-Butyl 7-(4-chlorophenyl)-2,3-dimethyl-5-oxo-2,3,7,8-tetrahydro-3,8a-epidioxypyrano[3,2-c]pyridine-6(5H)-carboxylate (**10d**)*

White solids in 84% yield, mp: 153–155 °C (ethyl acetate–hexane); IR (KBr) ν_{max} = 3075, 2982, 2935, 1770, 1722, 1643, 1492, 1359, 1288, 1151, 1001 cm^{-1}; ^1H NMR (600 MHz, $CDCl_3$) δ 7.16 (ddd, J = 7.5, 5.1, 2.8 Hz, 3H), 7.05–6.95 (m, 2H), 5.35 (t, J = 5.1 Hz) and

5.25 (s) (total 1H), 3.99 (dd, $J = 6.6$, 0.5 Hz) and 3.30 (d, $J = 6.3$ Hz) (total 1H), 2.37–2.25 (m, 2H), 1.29 (d, $J = 3.9$ Hz) and 1.24 (d, $J = 12.5$ Hz) (total 12H), 0.52 (d, $J = 6.6$ Hz, 3H); ^{13}C NMR (151 MHz, $CDCl_3$) δ 159.9, 159.6, 151.4 (duplicated), 139.5, 138.1, 138.0, 137.7, 135.0, 133.9, 133.4 (duplicated), 128.6 (duplicated), 127.3 (duplicated), 94.6 (duplicated), 84.4 (duplicated), 78.3, 76.1, 75.6, 73.0, 55.5 (duplicated), 35.5, 35.2, 31.5, 27.6 (duplicated), 17.3, 16.9 (duplicated), 14.6, 14.1. Anal. Calcd for $C_{21}H_{24}ClNO_6$: C, 59.79; H, 5.73; N, 3.32. Found: C, 60.10; H, 5.70; N, 3.28.

5.2.37. 3-Methyl-2-(4-nitrophenyl)-2,3,7,8-tetrahydro-3,8a-epidioxychromen-5(6H)-one (**13a**)

White solids in 96% yield, mp: 153–154 °C (ethyl acetate–hexane); IR (KBr) $\nu_{max} = 3074, 2943, 2881, 1701, 1626, 1606, 1519, 1348, 1274, 1109, 1049$ cm^{-1}; ^{1}H NMR (400 MHz, $CDCl_3$) δ 8.19–8.13 (m, 2H), 7.25 (dd, $J = 6.7$, 1.8 Hz, 2H), 6.99 (s, 1H), 5.30 (s, 1H), 2.59 (dd, $J = 8.6$, 5.4 Hz, 2H), 2.19 (dd, $J = 5.1$, 3.4 Hz, 2H), 2.04 (d, $J = 5.1$ Hz, 2H), 1.37 (s, 3H); ^{13}C NMR (101 MHz, $CDCl_3$) δ 193.4, 148.2, 142.8, 140.1, 135.3, 129.9, 128.3, 123.5, 123.3, 98.6, 79.9, 77.6, 38.5, 29.9, 18.2, 17.7. Anal. Calcd for $C_{16}H_{15}NO_6$: C, 60.57; H, 4.77; N, 4.41. Found: C, 60.77; H, 4.51; N, 4.35.

5.2.38. 2-(4-Methoxyphenyl)-3-methyl-2,3,7,8-tetrahydro-3,8a-epidioxychromen-5(6H)-one (**13b**)

White solids in 97% yield, mp: 130–131 °C (ethyl acetate–hexane); IR (KBr) $\nu_{max} = 2995, 2962, 2881, 1697, 1608, 1514, 1383, 1246, 1178, 1028$ cm^{-1}; ^{1}H NMR (400 MHz, $CDCl_3$) δ 7.08 (s, 1H), 7.00–6.94 (m, 2H), 6.85–6.75 (m, 2H), 5.13 (s, 1H), 3.77 (s, 3H), 2.64–2.47 (m, 2H), 2.24–2.12 (m, 2H), 2.08–1.91 (m, 2H), 1.31 (s, 3H); ^{13}C NMR (101 MHz, $CDCl_3$) δ 193.9, 159.9, 139.9, 136.6, 128.6, 127.8, 113.7, 98.7, 80.6, 78.1, 55.2, 38.6, 30.1, 18.2, 17.81. Anal. Calcd for $C_{17}H_{18}O_5$: C, 67.54; H, 6.00. Found: C, 67.22; H, 5.92.

5.2.39. 3-Methyl-2-(4-nitrophenyl)-7-phenyl-2,3,7,8-tetrahydro-3,8a-epidioxychromen-5(6H)-one (**13c**)

White solids in 94% yield, mp: 175–176 °C (ethyl acetate–hexane); IR (KBr) $\nu_{max} = 3070, 2937, 2895, 1685, 1616, 1521, 1348, 1263, 1182, 1028$ cm^{-1}; ^{1}H NMR (400 MHz, $CDCl_3$) δ 8.18 (ddt, $J = 11.1$, 9.2, 2.1 Hz, 2H), 7.38 (dd, $J = 10.1$, 4.6 Hz, 2H), 7.34–7.21 (m, 5H), 7.07 (d, $J = 11.7$ Hz, 1H), 5.34 (d, $J = 15.3$ Hz, 1H), 3.39–3.27 (m, 1H), 2.90 (ddd, $J = 18.1$, 3.8, 1.9 Hz, 1H), 2.81–2.68 (m, 1H), 2.57–2.41 (m) and 2.32–2.21 (m) (total 2H), 1.41 (d, $J = 9.5$ Hz, 3H); ^{13}C NMR (101 MHz, $CDCl_3$) δ 193.0, 148.2, 142.6, 141.5, 139.4, 135.8, 135.5, 129.03 (duplicated), 128.5 (duplicated), 127.43 (duplicated), 126.58 (duplicated), 123.6 (duplicated), 98.4, 98.7, 80.2, 79.4, 77.8, 46.1 (duplicated), 37.1 (duplicated), 36.5, 35.8, 17.7 (duplicated). Anal. Calcd for $C_{22}H_{19}NO_6$: C, 67.17; H, 4.87; N, 3.56. Found: C, 66.92; H, 4.56; N, 3.48.

5.2.40. 2-(4-Methoxyphenyl)-3-methyl-7-phenyl-2,3,7,8-tetrahydro-3,8a-epidioxychromen-5(6H)-one (**13d**)

White solids in 96% yield, mp: 175–176 °C (ethyl acetate–hexane); IR (KBr) $\nu_{max} = 3064, 2935, 2837, 1787, 1614, 1514, 1377, 1247, 1176, 1033$ cm^{-1}; ^{1}H NMR (400 MHz, $CDCl_3$) δ 7.40–7.32 (m, 2H), 7.32–7.21 (m, 3H), 7.16 (d, $J = 17.8$ Hz, 1H), 7.05–6.98 (m, 2H), 6.89–6.79 (m, 2H), 5.17 (d, $J = 13.9$ Hz, 1H), 3.79 (s, 3H), 3.51–3.41 (m) and 3.36–3.24 (m) (total 1H), 2.92–2.82 (m, 1H), 2.75–2.63 (m, 1H), 2.51–2.38 (m) and 2.23 (dd, $J = 14.0$, 13.2 Hz) (total 2H), 1.35 (d, $J = 8.6$ Hz, 3H); ^{13}C NMR (101 MHz, $CDCl_3$) δ 193.4, 193.0, 160.0, 141.8 (duplicated), 139.2 (duplicated), 137.1, 136.8, 128.9, 128.6 (duplicated), 127.78 (duplicated), 127.2 (duplicated), 126.5, 113.8 (duplicated), 98.5, 98.3, 81.0, 80.1, 78.3, 78.1, 55.2, 46.3 (duplicated), 37.3 (duplicated), 36.4, 36.0, 17.8 (duplicated). Anal. Calcd for $C_{23}H_{22}O_5$: C, 73.00; H, 5.86. Found: C, 72.93; H, 5.56.

6. Biological testing assay

6.1. Cell line

Established *in vitro*, human leukemia cell line: MV4-11 (biphenotypic B myelomonocytic leukemia) was used. This line was obtained from American Type Culture Collection (Rockville, Maryland, USA) and is being maintained at the Institute of Immunology and Experimental Therapy, Wroclaw, Poland.

MV4-11 cells were cultured in the RPMI 1640 medium (Gibco, Scotland, UK) supplemented with 2 mM L-glutamine and 1.0 mM sodium pyruvate, 10% fetal bovine serum (all from Sigma–Aldrich Chemie GmbH, Steinheim, Germany), 100 units/ml penicillin, and 100 μg/mL streptomycin (both from Polfa, Tarchomin S.A., Poland). The cell line was grown at 37 °C with 5% CO_2 humidified atmosphere.

HCT116 and A549 cells were cultured in the RPMI 1640 + OptiMEM (50:50) medium (Gibco, Scotland, UK) supplemented with 2 mM L-glutamine and 5% fetal bovine serum (all from Sigma–Aldrich Germany), BALB/3T3 cells were cultured in Dulbecco medium (IIET) supplemented with 2 mM L-glutamine and 1.0 mM sodium pyruvate, 10% fetal bovine serum (all from Sigma–Aldrich Germany). All culture medium was supplemented with 100 units/ml penicillin and 100 μg/mL streptomycin (both from Polfa, Tarchomin S.A., Poland). All cell lines were grown at 37 °C with 5% CO_2 humidified atmosphere.

6.2. Antiproliferative assay in vitro

Test solutions of the compounds tested (1 mg/ml) were prepared by dissolving the substances in 100 μl of DMSO completed with 900 μl of tissue culture medium. Afterward, the tested compounds were diluted in culture medium to reach the final concentrations of 10, 1, 0.1, 0.01 μg/mL.

Twenty four hours prior to the addition of the tested compounds, the cells were plated in 96-well plates (Sarstedt, Germany) at a density of 1×10^4 cells per well. The assay was performed after 72 h of exposure to varying concentrations of the tested agents. The *in vitro* cytotoxic effect of all agents was examined using the MTT or SRB assay [32].

The results were calculated as an IC_{50} (inhibitory concentration 50) – the dose of tested agent which inhibits proliferation of 50% of the cancer cell population. IC values were calculated for each experiment separately and mean values SD are presented in Tables 1 and 2. Each compound in each concentration was tested in triplicate in a single experiment, which was repeated 3–5 times.

6.3. MTT assay

This technique was applied for the cytotoxicity screening against MV4-11 leukemia cells growing in suspension culture. An assay was performed after 72-h exposure to varying concentrations (from 0.001 to 10 g/ml) of the tested agents. For the last 3–4 h of incubation 20 μl of MTT solution were added to each well (MTT: 3-(4,5-dimethylthiazol-2-yl)-2,5-diphenyl tetrazolium bromide; stock solution: 5 mg/ml, Sigma, Germany). The mitochondria of viable cells reduce the pale yellow MTT to a navy blue formazan: the more viable cells are present in well, the more MTT will be reduced to formazan. When incubation time was completed, 80 μl of the lysing mixture were added to each well (lysing mixture: 225 ml dimethylformamide, POCh, Gliwice, Poland, 67.5 g sodium dodecyl sulfate, Sigma, Germany, and 275 ml of distilled water). After 24 h, when formazan crystals had been dissolved, the optical densities of the samples were read on an Multiskan RC photometer at 570 nm wavelength.

6.4. SRB assay

This technique was applied for the cytotoxicity screening against cells growing in adherent culture (A549, HCT116 and Balb/3T3). The details of this technique were described by Skehan [33]. The cytotoxicity assay was performed after 72-h exposure of the cultured cells to varying concentrations (from 0.01 to 10 g/ml) of the tested agents. The cells attached to the plastic were fixed by gently layering cold 50% TCA (trichloroacetic acid, POCh, Poland) on the top of the culture medium in each well. The plates were incubated at 4 °C for 1 h and then washed five times with tap water. The background optical density was measured in the wells filled with culture medium, without the cells. The cellular material fixed with TCA was stained with 0.4% sulforhodamine B (SRB, Sigma, Germany) dissolved in 1% acetic acid (POCh, Gliwice, Poland) for 30 min. Unbound dye was removed by rinsing (4×) with 1% acetic acid. The protein-bound dye was extracted with 10 mM unbuffered Tris base (Sigma, Germany) for determination of optical density (at 540 nm) in a computer-interfaced, 96-well microtiter plate reader Multiskan RC photometer (Labsystems, Helsinki, Finland).

6.5. Activity against P. falciparum

Experimental procedure *in vitro* activity testing against erythrocytic stages of *P. falciparum* was performed on the basis of the reported method [34].

6.6. In vitro cytotoxicity against L6 cells

Assays were performed on the basis of the reported method [34].

Acknowledgments

We are grateful to Okayama University for its support and to the Advanced Science Research Center for the NMR experiments, EA by Mr. M. Kobayashi and Ms. M. Kosaka, and X-ray analyses by Dr. H. Ota. We are thankful to Prof. S. Nakashima and Prof. J. Nokami (Okayama University of Science) for HRMS analyses, and Prof. J. Futami for UV analyses. This study was partially supported by the Adaptable and Seamless Technology Transfer Program of JST.

Appendix A. Supplementary data

Supplementary data related to this article can be found at http://dx.doi.org/10.1016/j.ejmech.2013.08.008.

References

[1] A.L. Couffignal, M. Lapeyre-Mestre, C. Bonhomme, R. Bugat, J.L. Montastruc, Adverse effects of anticancer drugs: apropos of a pharmacovigilance study at a specialized oncology institution, Therapie 55 (2000) 635–641.
[2] G.M. Cragg, D.J. Newman, Developments and future trends in anticancer natural products drug discovery, in: G.M. Cragg, D.G.I. Kingston, D.J. Newman (Eds.), Anticancer Agents from Natural Products, second ed., CRC Press, Boca Raton, FL, 2012, pp. 699–727.
[3] M.E. Wall, M.C. Wani, Camptothecin and taxol: discovery to clinic – thirteenth Bruce F. Cain memorial award lecture, Cancer Res. 55 (1995) 753–760.
[4] C. Jaquet, H.R. Stohler, J. Chollet, W. Peters, Antimalarial activity of the bicyclic peroxide Ro 42-1611 (arteflene) in experimental models, Trop. Med. Parasitol. 45 (1994) 266–271.
[5] M.D. Bachi, E.E. Korshin, R. Hoos, A.M. Szpilman, P. Ploypradith, S. Xie, T.A. Shapiro, G.H. Posner, A short synthesis and biological evaluation of potent and nontoxic antimalarial bridged bicyclic β-sulfonyl-endoperoxides, J. Med. Chem. 46 (2003) 2516–2533.
[6] K.I. Kimura, Y. Sakamoto, N. Fujisawa, S. Uesugi, N. Aburai, M. Kawada, S.I. Ohba, T. Yamori, E. Tsuchiya, H. Koshino, Cleavage mechanism and antitumor activity of 3,6-epidioxy-1,10-bisaboladiene isolated from edible wild plants, Bioorg. Med. Chem. 20 (2012) 3887–3897.
[7] G.H. Posner, L.E. Woodard, L.R. David, D.K. Moon, B.T. Mott, Preparation of trioxane monomer and dimer derivatives for use in the treatment of malaria and cancer, PCT Int. Appl. (2010), WO 2010135427 A2 20101125.
[8] P. Ploypradith, Development of artemisinin and its structurally simplified trioxane derivatives as antimalarial drugs, Acta Trop. 89 (2004) 329–342.
[9] Y. Dong, S. Wittlin, K. Sriraghavan, J. Chollet, S.A. Charman, W.N. Charman, C. Scheurer, H. Urwyler, J.S. Tomas, C. Snyder, D.J. Creek, J. Morizzi, M. Koltun, H. Matile, X. Wang, M. Padmanilayam, Y. Tang, A. Dorn, R. Brun, J.L. Vennerstrom, The structure–activity relationship of the antimalarial ozonide arterolane (OZ277), J. Med. Chem. 53 (2010) 481–491.
[10] S.R. Meshnick, T.E. Taylor, S. Kamchonwongpaisan, Artemisinin and the antimalarial endoperoxides: from herbal remedy to targeted chemotherapy, Microbiol. Rev. 60 (1997) 301–315.
[11] J.N. Cumming, P. Ploypradith, G.H. Posner, Antimalarial activity of artemisinin (qinghaosu) and related trioxanes: mechanism(s) of action, Adv. Pharmacol. 37 (1997) 253–297.
[12] W. Jefford, Peroxidic antimalarials, Adv. Drug Res. 29 (1997) 271–325.
[13] A. Robert, B. Meunier, Characterization of the first covalent adduct between artemisinin and a heme model, J. Am. Chem. Soc. 119 (1997) 5968–5969.
[14] A. Robert, B. Meunier, Heme as trigger and target for trioxane-containing antimalarial drugs, Acc. Chem. Res. 43 (2010) 1444–1451.
[15] P.L. Olliaro, R.K. Haynes, B. Meunier, Y. Yuthawong, Possible modes of action of the artemisinin-type compounds, Trends Parasitol. 17 (2001) 122–126.
[16] P.M. O'Neill, J. Chadwick, S.L. Rawe, Biomimetic Fe(II) chemistry and synthetic studies on antimalarial and antitumour endoperoxides, Chem. Peroxides 2 (2006) 1279–1346.
[17] J.P. Jeyadevan, P.G. Bray, J. Chadwick, A.E. Mercer, A. Byrne, S.A. Ward, B.K. Park, D.P. Williams, R. Cosstick, J. Davies, A.P. Higson, E. Irving, G.H. Posner, P.M. O'Neill, Antimalarial and antitumor evaluation of novel C-10 non-acetal dimers of 10β-(2-hydroxyethyl)deoxoartemisinin, J. Med. Chem. 47 (2004) 1290–1298.
[18] P.M. O'Neill, G.H. Posner, A medicinal chemistry perspective on artemisinin and related endoperoxides, J. Med. Chem. 47 (2004) 2945–2964.
[19] G.H. Posner, J. D'Angelo, P.M. O'Neill, A. Mercer, Anticancer activity of artemisinin-derived trioxanes, Expert Opin. Ther. Patents 16 (2006) 1665–1672.
[20] I.-H. Paik, S. Xie, T.A. Shapiro, T. Labonte, A.A. Narducci Sarjeant, A.C. Baege, G.H. Posner, Second generation, orally active, antimalarial, artemisinin-derived trioxane dimers with high stability, efficacy, and anticancer activity, J. Med. Chem. 49 (2006) 2731–2734.
[21] D.M. Rubush, M.A. Morges, B.J. Rose, D.H. Thamm, T. Rovis, An asymmetric synthesis of 1,2,4-trioxane anticancer agents via desymmetrization of peroxyquinols through a Brønsted acid catalysis cascade, J. Am. Chem. Soc. 134 (2012) 13554–13557.
[22] T. Yamori, A. Matsunaga, S. Sato, K. Yamazaki, A. Komi, K. Ishizu, I. Mita, H. Edatsugi, Y. Matsuba, K. Takezawa, O. Nakanishi, H. Kohno, Y. Nakajima, H. Komatsu, T. Andoh, T. Tsuruo, Potent antitumor activity of MS-247, a novel DNA minor groove binder, evaluated by an in vitro and in vivo human cancer cell line panel, Cancer Res. 59 (1999) 4042–4049.
[23] T. Yamori, Panel of human cancer cell lines provides valuable database for drug discovery and bioinformatics, Cancer Chemother. Pharmacol. 52 (Suppl. 1) (2003) 74–79.
[24] W. Peng, T. Hirabaru, H. Kawafuchi, T. Inokuchi, Substituent-controlled electrocyclization of 2,4-dienones: synthesis of 2,3,6-trisubstituted 2*H*-pyran-5-carboxylates and their transformations, Eur. J. Org. Chem. (2011) 5469–5474.
[25] M.I. Hossain, E. Shaban, T. Ikemi, W. Peng, T. Hirabaru, H. Kawafuchi, T. Inokuchi, Annulation of 2*H*-pyran onto 1-oxa- or 1-azacyclohexane-2,4-diones and their analogues via sequential condensation with α-substituted enals and 6π-electrocyclization, Bull. Chem. Soc. Jpn. 86 (2013) 870–879.
[26] J.A. Michael, J.H. Susan, G.N. Christopher, B.T. John, C.D.T. Sylvie, Synthesis of 6-aryl-4-hydroxypiperidin-2-ones and a possible application to the synthesis of a novel HMG-CoA reductase inhibitor, Heterocycles 28 (1989) 1015–1035.
[27] D. Kong, T. Yamori, JFCR39, a panel of 39 human cancer cell lines, and its application in the discovery and development of anticancer drugs, Bioorg. Med. Chem. 20 (2012) 1947–1951.
[28] P.A. Berman, P.A. Adams, Artemisinin enhances heme-catalyzed oxidation of lipid membranes, Free Radic. Biol. Med. 22 (1997) 1283–1288.
[29] P.T. Mpiana, B.K. Mavakala, Z.-W. Yu, Interaction of artemisinin based antimalarial drug with hemin in water-DMSO mixture, Int. J. Pharmacol. 3 (2007) 302–310.
[30] K. Dutta, S. Mukhopadhyay, S. Bhattacharjee, B. Chaudhuri, Chemical oxidation of methylene blue using a Fenton-like reaction, J. Hazard. Mater. 84 (2001) 57–71.
[31] N. Lu, L. Yi, Q. Deng, J. Li, Z. Gao, H. Li, The interaction between desferrioxamine and hemin: a potential toxicological implication, Toxicol. in Vitro 26 (2012) 732–735.
[32] R.B. Michael, D.P. Kenneth, Some practical considerations and applications of the National Cancer Institute in vitro anticancer drug discovery screen, Drug Dev. Res. 34 (1995) 91–109.
[33] P. Skehan, R. Storeng, D. Scudiero, A. Monks, J. McMahon, D. Vistica, J.T. Warren, H. Bokesch, S. Kenney, M.R. Boyd, New colorimetric cytotoxicity assay for anticancer-drug screening, J. Natl. Cancer Inst. 82 (1990) 1107–1112.
[34] W.-J. Lu, K.J. Wicht, L. Wang, K. Imai, Z.-W. Mei, M. Kaiser, I.E.T.E. Sayed, T.J. Egan, T. Inokuchi, Synthesis and antimalarial testing of neocryptolepine analogues: addition of ester function in SAR study of 2,11-disubstituted indolo [2,3-*b*]quinolones, Eur. J. Med. Chem. 64 (2013) 498–511.